BASIC PRINCIPLES OF MR IMAGING

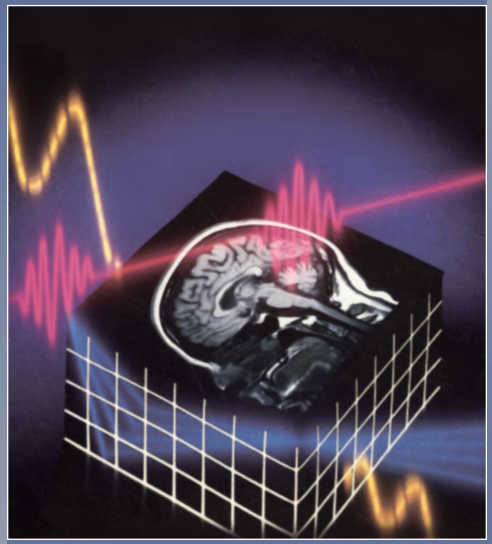

GE Medical Systems
Training in Partnership

NAVIGATION

NOTES ON USING THIS ELECTRONIC DOCUMENT

In addition to the built-in features of the Adobe Acrobat™ Reader software, several different types of navigation devices have been added to this electronic document. These "buttons" will appear at various points within the document and allow you to jump to specific reference areas. A brief explanation of these buttons is illustrated below:

CONTINUED

This button will appear in the lower right corner of a screen containing text. It means that the next few pages are going to be images or illustrations. By clicking the cursor on this button you will be taken to the next page in the current text chain.

(FIG. 58)

This button appears within the text itself. If a particular figure (either an illustration or an image) is being referenced — then clicking the cursor on the colored text will take you to the page containing that particular figure.

BACK

This button works in tandem with the (FIG) button. It appears on the bottom of a page containing an illustration or image. Clicking on it will return you to the portion of text that the figure was referenced from.

Basic Principles of Magnetic Resonance Imaging

Paul J. Keller, Ph.D.

Department of Magnetic Resonance Research
Barrow Neurologic Institute
St. Joseph's Hospital and Medical Center
Phoenix, AZ 85013

Table of Contents

FOREWORD

For many MR users, "*NMR: A Perspective on Imaging*" had been the first exposure to magnetic resonance. This highly successful primer was reprinted twice, and is now permanently out of print. Why not reprint it a third time? After all, MR physics cannot have changed a great deal over the past six years. True, but our understanding has, and so has the significance of many of its aspects. In fact, the technology has made tremendous leaps forward since the beginning of this decade, when MR entered the phase of initial clinical trials. Also, the understanding of critical performance criteria has become more sophisticated, paralleling advances in instrumentation. New methodology, such as rapid imaging, 3D acquisition, variable bandwidth and many more are terms and techniques which confront the MR novice.

Dr. Paul Keller, the author of the current primer, has a profound understanding of magnetic resonance and its many applications, and many years of hands-on experience. Beyond this, he has the rare ability to teach MR physics (a term for which the average radiologist has an innate aversion) in a non-threatening and lucid manner.

Felix W. Wehrli
Milwaukee, Wisconsin
June, 1988

CONTINUED

CHAPTER 1

Basics of the Magnetic Resonance Phenomenon

Over the past several years, magnetic resonance imaging (MRI) has developed into a very powerful and versatile diagnostic technique in medicine. This, in turn, led to the proliferation of MRI equipment and spurred massive amounts of research.

What are the reasons for all of this excitement? Unlike x-ray based modalities such as computed tomography (CT) scanning, MRI is a non-invasive technique which does not employ ionizing radiation. Further, the only tissue-specific parameter that can be determined with x-rays is electron density, which does not vary greatly from one soft tissue to another, and often necessitates the injection of contrast media.

In MRI, on the other hand, there is a multitude of tissue parameters which can affect MR signals. The two most significant, the relaxation times, cover a wide range of values in various normal and pathologic tissues. In addition, signal acquisition parameters can be manipulated in a variety of ways, enabling the user to control image contrast.

This primer has been written for physicians and technologists who seek an introduction to the mechanisms underlying MRI.

The first section discusses the physics of magnetic resonance of atomic nuclei. The second section introduces the techniques employed for exploiting the MR phenomenon for the purpose of image formation.

CONTINUED

A few basic physical equations are provided, but the text can be largely understood without them. Many of the figures and much of the glossary have been borrowed from an earlier primer published by GE Medical Systems.

Spins in a Magnetic Field

During the development of the quantum mechanical concept of atomic structure, it became apparent that most nuclei possess a property called spin angular momentum, which is the basis of nuclear magnetism. In the following, let us construct an intuitive view of the consequences and manipulation of nuclear spin. (**REFS. 14-15**).

(**FIG. 1**) depicts a nucleus spinning around an axis. Since atomic nuclei are charged, the spinning motion causes a magnetic moment which is colinear with the direction of the spin axis. The magnetic moment acts similar to a bar magnet having north and south poles. The strength of this magnetic moment is a property of the type of nucleus and determines the detection sensitivity of MR (**TABLE 1**). ^{1}H nuclei (protons) possess the strongest magnetic moment, which, together with the high biological abundance of hydrogen, makes it the nucleus of choice for MR imaging.

Consider a collection of protons as in (**FIG. 2**). In the absence of an externally applied magnetic field, the individual magnetic moments have no preferred orientation. However, if an externally supplied magnetic field (denoted B_0) is imposed, there is a tendency for the magnetic moments to align with the external field, just like bar magnets would do. Nuclear magnetic moments in this situation may adopt one of two possible orientations: alignment parallel or anti-parallel to B_0 (**FIG. 3**). Thus, depending on their orientation, we can define two groups or populations of spins. Alignment parallel to B_0 is the lower energy orientation and is thus preferred, while the anti-parallel alignment is the higher energy state (**FIG. 4**). For the sake of completeness, it should be mentioned that this situation of only two allowed states is true only for nuclei whose "magnetic spin quantum number" is equal to 1/2. This includes ^{1}H, ^{13}C, ^{19}F, ^{31}P and others.

CONTINUED

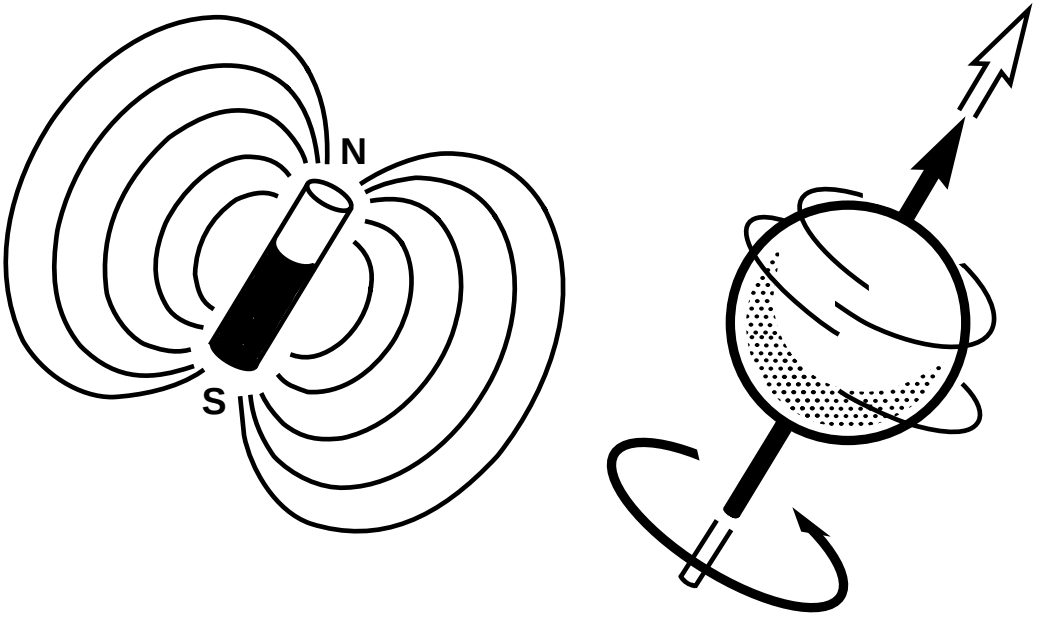

FIGURE 1 – The magnetic dipole and associated spin of certain nuclei may be compared to a common bar magnet with rotation about the dipole axis.

Nucleus	Natural Abundance %	Gamma[1] Hz / Gauss	Relative[2] Sensitivity
^{1}H	99.98	4257	1
^{2}H	0.015	653	0.0097
^{13}C	1.1	1071	0.016
^{19}F	100	4005	0.830
^{23}Na	100	1126	0.093
^{31}P	100	1723	0.066
^{39}K	93.1	199	0.0005

TABLE 1 – Magnetic Resonance properties of some biochemically important nuclei

1 Gamma is directly proportional to the magnitude of the nuclear magnetic moment.
2 At constant field for equal numbers of nuclei.

BACK

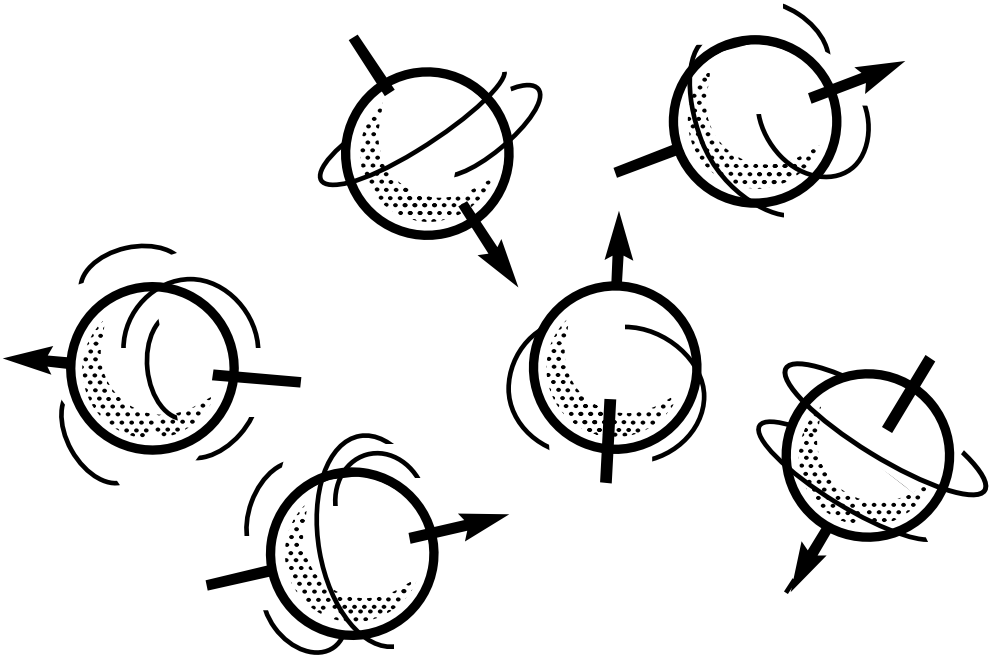

FIGURE 2 – In the absence of an externally applied magnetic field, the nuclear magnetic moments have random orientations.

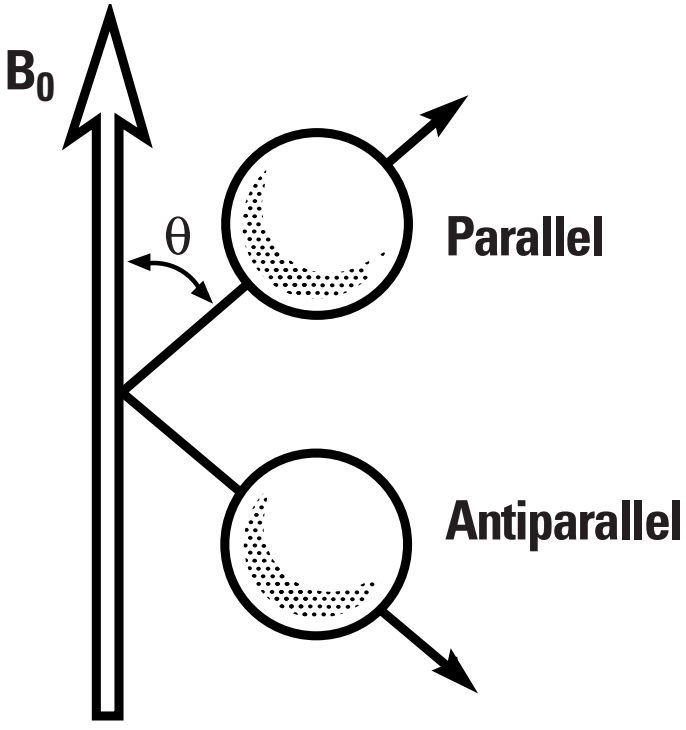

FIGURE 3 – In the presence of an externally applied magnetic field (B_0) spins are constrained to adopt one of two orientations with respect to B_0. These orientations are denoted as parallel and anti-parallel.

BACK

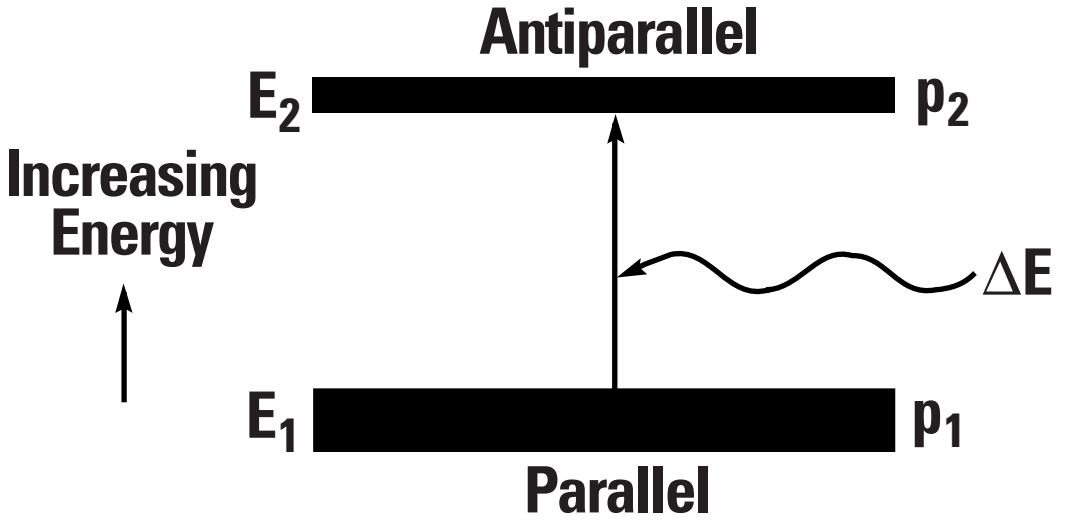

FIGURE 4 – The parallel spin orientation is a lower energy state than anti parallel. Since spins must adopt one of the two orientations, there are two populations (P1, P2) of spins corresponding to two energy levels (E1, E2). E2 is greater than E1, causing P1 to be greater than P2. Some spins of P1 may move to P2 if the exact amount of energy equal to E2 - E1 = ΔE is supplied to the system.

BACK

Other magnetically active nuclei, e.g. ^{2}H and ^{23}Na, are allowed more than two orientations.

One might think that all of the spins would occupy the lower energy state. This would be true at a temperature of absolute zero, but we are interested in the situation under somewhat more temperate conditions. Since the energy difference (ΔK) between the two states is very small, thermal energy alone causes the two states to be *almost* equally populated (the population ratio is approximately 100,000 to 100,006). The remaining population difference results in a net bulk magnetization aligned parallel to B_0. It is only this net magnetization arising from a small population difference which is detectable by MR techniques.

Let's examine this net magnetization in more detail. The individual spins do not align exactly parallel (or antiparallel) to B_0, but at an angle to B_0 (**FIG. 5A**). The spin associated with the magnetic moment causes the moment to precess around the axis of B_0. This is analogous to the case of a spinning top: the top precesses about the axis defined by the pull of gravity. This precession then defines the surface of a cone.

Now we may refine our picture of how a large collection of spins yields a net bulk magnetization. (**FIG. 5B**) shows a model of the situation at any given instant. Here, each of the vectors (arrows) represents an individual spin. Since we already know that there are more spins aligned with B_0 than against B_0, the contribution of the bottom cone cancels out, leaving only the excess spins of the top cone to consider. Any given vector on the top cone could be described by its components perpendicular to and parallel to B_0. Clearly, for a large enough collection of spins randomly distributed on the surface of the cone, individual components perpendicular to B_0 will cancel each other. This leaves only the contributions parallel to B_0 explaining why the bulk net magnetization is indeed parallel to B_0.

We may next inquire how fast the individual spins precess on the surface of the cone.

CONTINUED

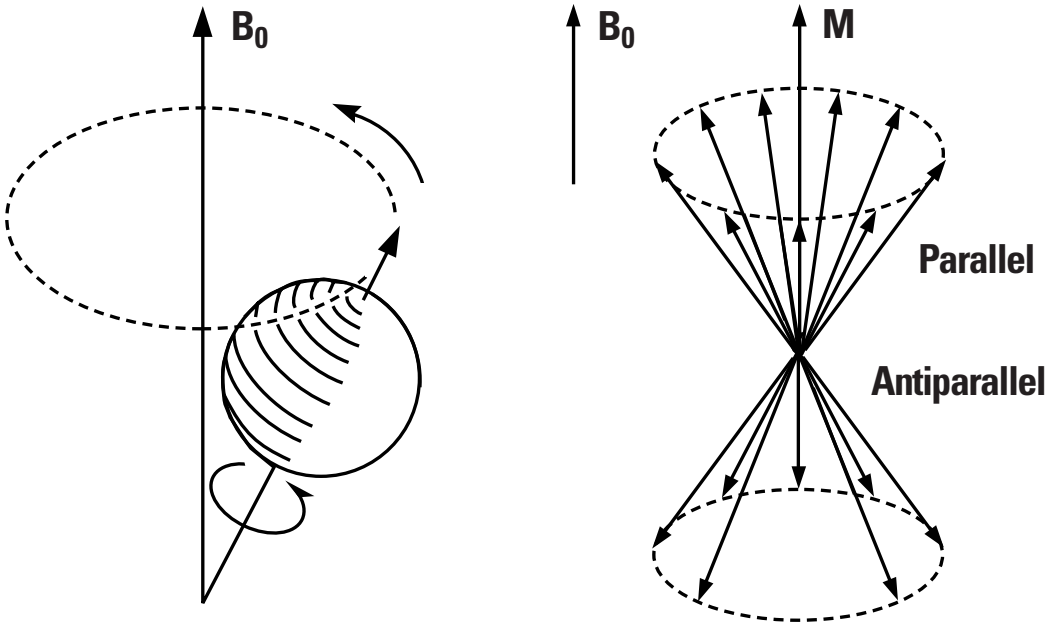

FIGURE 5 – (A) As seen previously in FIGURE 3, the spin axes do not actually align parallel or anti-parallel to B_0, but at an angle to B_0. This causes the spin axis to precess like a top around B_0, thus describing the surface of a cone. (B) This is a depiction of a collection of spins at any given instant. The vector (arrow) M represents the bulk net magnetization which results from the sum of the contributions from each of the spins.

BACK

This precessional frequency is given by a beautifully simple relationship called the Larmor equation, expressed as:

$$\gamma B_0 = F \quad [1]$$

F is the precessional frequency, B_0 is the strength of the magnetic field, and gamma (γ) is related to the strength of the magnetic moment for the type of nucleus considered.

For our purposes:

$$\gamma_H = 4257 \text{ Hz / Gauss}$$

Thus at 1.5 Tesla (= 15,000 Gauss) 4257 Hz/ Gauss x 15,000 Gauss = 63,855,000 Hertz = 63.855 Megahertz (MHz).

Correspondingly, at 0.5 Tesla, the Larmor frequency for protons is 21.285 MHz. We see that the rate of precession is very fast.

Re-examination of (**FIG. 4**) shows that since energy is proportional to frequency, ΔE may be defined in terms of the frequency of radiation which is necessary to induce transitions of spins between the two energy levels. For reasons which are not obvious without delving more deeply into physics, the frequency corresponding to ΔE is again the Larmor frequency.

The Effect of Radiofrequency (RF) Pulses

In order to detect a signal, a condition of resonance needs to be established. The term "resonance" implies alternating absorption and dissipation of energy. Energy absorption is caused by RF perturbation, and energy dissipation is mediated by relaxation processes (*Next Section*). Simply put, as mentioned above, irradiation of a collection of spins in an exogenous magnetic field with RF energy at the Larmor frequency induces transitions between the two energy levels. RF energy at other frequencies has no effect. That is the microscopic picture, but what can actually be observed for the macroscopic net magnetization?

CONTINUED

RF radiation, like all electromagnetic radiation, possesses electric and magnetic field components. We may consider the RF as another magnetic field (denoted as B_1) perpendicular to B_0, i.e. along a given axis in the transverse plane (**FIG. 6**). When the RF is turned on, the net magnetization vector begins to precess about the B_1 axis. Thus the net magnetization rotates from the longitudinal (Z) axis toward the transverse plane then toward the –Z axis, then to the other side of the transverse plane, and back to +Z and so on. If the RF is on for only a short period of time, the net magnetization is rotated by a certain angle away from the longitudinal axis; this angle is termed the *flip angle*. Intuitively, we understand that the flip angle is proportional to the duration of an RF pulse and the amplitude of the RF. As we will see, flip angles of 90° and 180° are of special importance in imaging.

Consider the situation immediately after a 90° pulse (**FIG. 7**). The net magnetization now lies in the transverse plane and begins to precess around the B_0 axis. The rate of this precession is just as calculated above—it is the Larmor frequency. Since this is macroscopic magnetization which is changing direction (rotating) over time, it can induce an alternating (AC) current in a coil of wire, and that current can be used to record the action of magnetization in the transverse plane. (**FIG. 8**) shows such a record. Note that it shows a sinusoidal oscillation at the Larmor frequency. Furthermore, the signal gets weaker with time. This is a free induction decay (or FID). Here "free" refers to the lack of the driving B_1 field at the time of observation; the signal which is induced in the receiver coil decays over time. The signal decay is due to a process known as relaxation.

Relaxation: The Return to Equilibrium

Returning briefly to the analogy of a bar magnet aligned with an external magnetic field, we may inquire about what happens if the bar magnet is turned away from this alignment. The bar magnet would naturally tend to realign itself with the field, but how rapidly would this occur?

CONTINUED

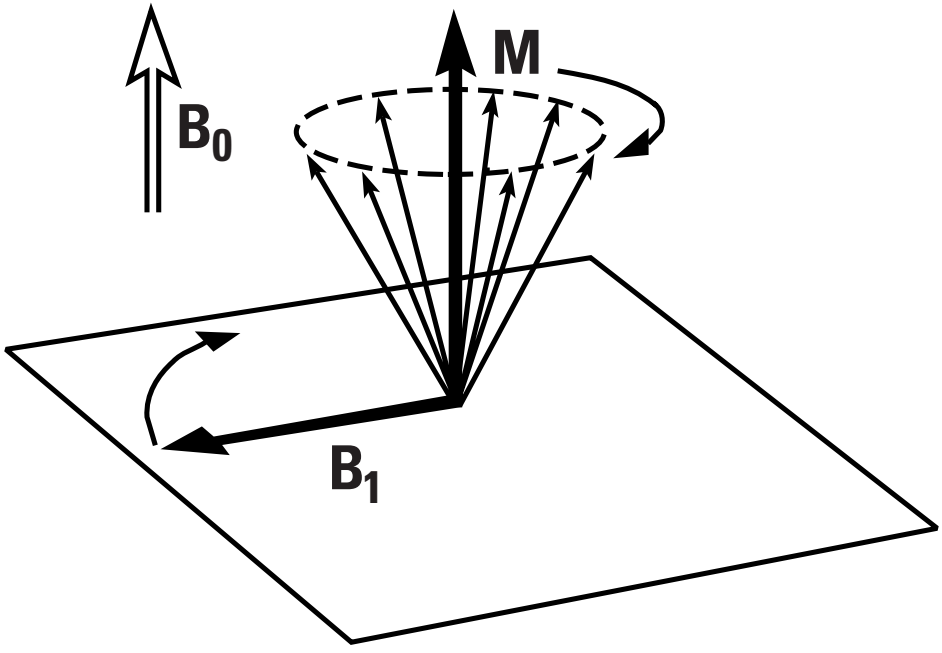

FIGURE 6 – RF energy at the Larmor frequency acts as a second magnetic field (B_1) which is perpendicular to B_0. When the RF is on, M rotates about B_1. As shown here, M is originally longitudinal and B_1 is turned on long enough to rotate M by 90° i.e.. into the transverse plane.

BACK

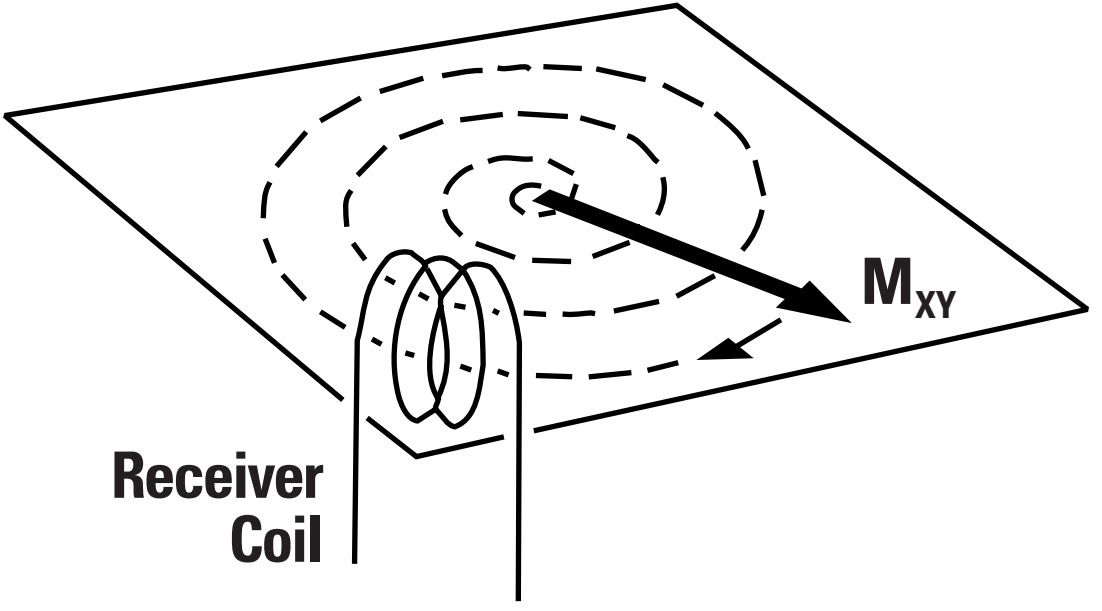

FIGURE 7 – Once in the transverse plane, M precesses (rotates) about B_0 at the Larmor frequency. This rotating magnetization can induce an AC current in the receiver coil. The transverse magnetization decays over time, which is represented by a decreasing length of the vector M.

BACK

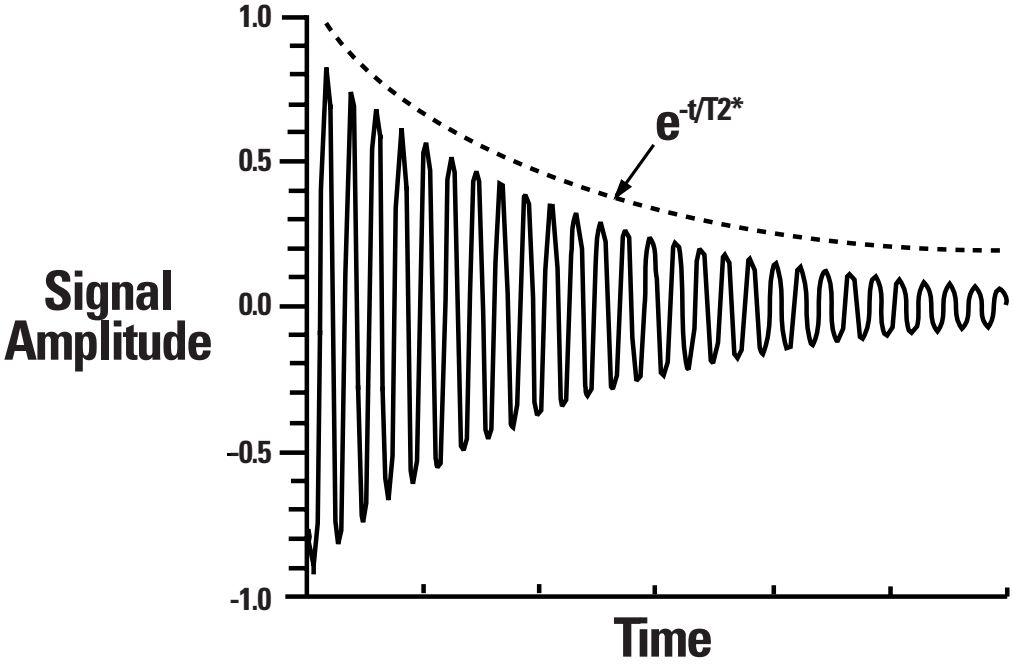

FIGURE 8 – A graph of the voltage (signal) induced in the receiver coil versus time. This waveform is termed a free induction decay (FID); it is an ex ponentially damped sine wave. The decay rate is characterized by the time constant T2*.

BACK

Would the return to equilibrium be linear or exponential with respect to time? For the bar magnet, the equilibrium orientation is in alignment with the external field. Once equilibrium conditions have been attained there is no further change unless the system is perturbed.

For the net magnetization arising from a collection of spins in an external field equilibrium is described by a vector of unit length parallel to B_0. We will see that it is appropriate to consider relaxation in the transverse plane independently of relaxation along the longitudinal axis.

Transverse Relaxation

Given that at equilibrium the net magnetization is longitudinal, it follows that the equilibrium magnetization in the transverse plane is zero. This is illustrated in (**FIG. 8**), showing the decay of the transverse magnetization to zero. This process is exponential (as opposed to linear). This is reminiscent of other natural processes, e.g. radioactive decay. As in radioactive decay one could define a quantity such as the half-life for the transverse magnetization. The relationship describing the decay is

$$[2] \quad M_{transverse} = M^0_{transverse}\, e^{-t/T2*}$$

Where $M^0_{transverse}$ is the initial amount of transverse magnetization, $M_{transverse}$ is the amount of transverse magnetization at any given time (**t**) after a pulse, **e** is approximately 2.7, and **T2*** characterizes the rate of decay.

$$\text{If } t = T2^*,\ M(T2^*) = M^0_{transverse} / e = M^0_{transverse} / 2.7 = 0.37\ M^0_{transverse}.$$

Hence, T2* is the time it takes for the transverse magnetization to decay to 37% of the initial value.

What mechanisms cause the observed decay of transverse magnetization? As shown in (**FIG. 9**), different components of the magnetization may precess at slightly different rates, a process known as “dephasing” in the transverse plane.

CONTINUED

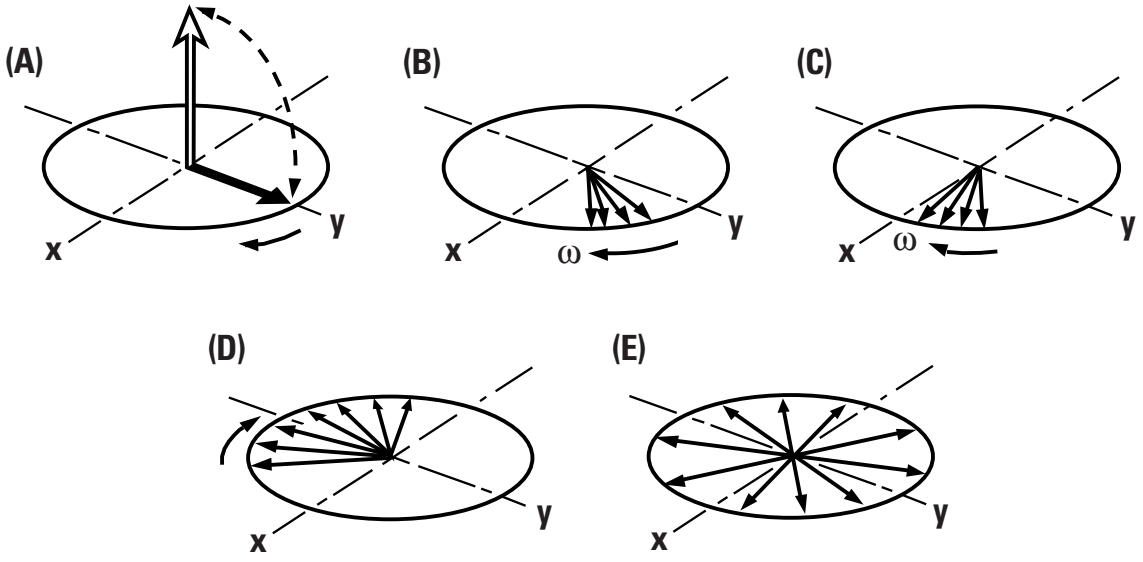

FIGURE 9 – (A) The B_1 field of the RF rotates M into the transverse plane. (B-E) The magnetization rotating in the transverse plane is actually the sum of the contributions from all of the spins in the excited sample. However, the spins at different points in the sample may not "feel" the same B_0 field due to B_0 inhomogeneity. This results in a range of precessional frequencies, causing the various components of M to spread apart over time. This loss of "phase coherence" eventually leads to self-cancellation of the signal.

BACK

Since the signal recorded is the sum of all the transverse components, sufficient dephasing will lead to complete cancellation of the signal. One of the major causes of this dephasing is B_0 inhomogeneity: spins at different locations are not exposed to exactly the same B_0 field, which in turn yields a range of Larmor frequencies. If one had a completely homogeneous B_0 field, dephasing would still occur, but much more slowly. Since many atomic nuclei and electrons are spins and possess magnetic moments, the microscopic local magnetic environment of a spin participating in the observed resonance is not precisely identical to those of the other observed spins. Additionally, these microscopic environments change very rapidly. This spatial and temporal variation of magnetic environments yields variation in the Larmor frequencies causing the slower dephasing This slower dephasing and concomitant signal decay is due to the physical properties of the system (or tissue) under investigation, and is denoted as T2 relaxation or spin-spin relaxation. Now it can be appreciated that T2* describes the decay rate observed due to the combination of spin-spin relaxation and B_0 inhomogeneity.

For many reasons it is useful to record signals which reflect T2 rather than T2* decay. Obviously, some sort of trick is necessary in order to accomplish this, since a perfectly homogeneous B_0 field is not attainable. The "trick" is called a spin-echo, and it is the basis for the majority of clinical MR imaging A pulse sequence is a set of RF pulses (and for imaging, field gradient pulses as introduced in the next section) of defined timing and amplitude which is usually repeated many times, each time resulting in collection of an MR signal. (**FIG. 10**) depicts an RF pulse sequence for a spin-echo. An initial 90° pulse yields a FID which decays as a function of T2*, then at a time TE/2 after the 90° pulse, a 180° RF pulse is applied. After the 180° pulse, a so-called "echo signal" forms, reaching its maximum amplitude at time TE after the initial 90° pulse. A second spin-echo can be obtained by applying another 180° pulse, and further echoes are possible with additional 180° pulses. Note that the echo-to-echo amplitudes decay as a function of T2 rather than T2*.

CONTINUED

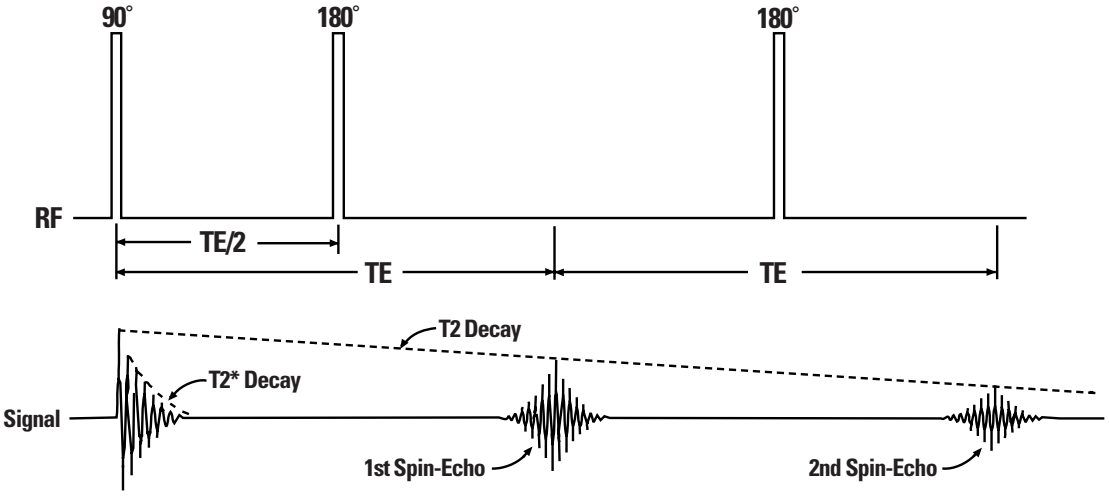

FIGURE 10 – A spin echo is generated by the application of a 90° RF pulse and, after a delay (TE/2), a 180° RF pulse. The peak of the echo occurs at time TE after the initial 90° pulse. Further echoes are obtainable with additional 180° pulses. The echo-to-echo decay rate is described by T2, which is much longer than T2*.

BACK

What causes the echoes to form, and how is the effect of B_0 inhomogeneity eliminated? The mechanism of spin- echo formation can be explained by reference to (**FIG. 11**). Consider transverse magnetization arising from two locations experiencing different values of B_0.

Transverse magnetization from the two locations will precess at different rates. This is symbolized with two vectors labeled as F (fast) and S (slow). Immediately after the 90° pulse, F and S are together (in phase) in the transverse plane. Both F and S begin to precess clockwise in the plane, but as time goes on F and S get further apart because of their different precessional rates. At this time, the 180° RF pulse is applied. Its effect is to rotate both F and S into mirror image locations relative to the 180° rotation axis. F and S now continue clockwise precession, with F *behind* S. At time (TE), however, F will catch up with S and both will be back in phase again. If there were many vectors with a wide range of precessional frequencies, they would all still come back into phase at time TE. In the section on imaging techniques it will become clear that the choices of TE and TR (time between repetitions of the entire pulse sequence) have a significant impact on signal and contrast of MR images. (**REF. 16**)

Longitudinal Relaxation

Up to this point, only relaxation in the transverse plane has been discussed. A separate process must exist which restores longitudinal magnetization to its equilibrium value.

Immediately after a 90° pulse, the net magnetization vector lies in the transverse plane. Therefore the amount of longitudinal magnetization is zero. If we examine the amount of longitudinal magnetization present at various times after the 90° pulse, we find that it builds up exponentially from zero to approach the equilibrium value, which is a function of the number of spins present, temperature and magnetic field strength (**FIG. 12**). The process by which this occurs is denoted as *spin-lattice relaxation* or *T1 relaxation*. In terms of the two energy levels in (**FIG. 4**), a 90° pulse makes the spin populations equal.

CONTINUED

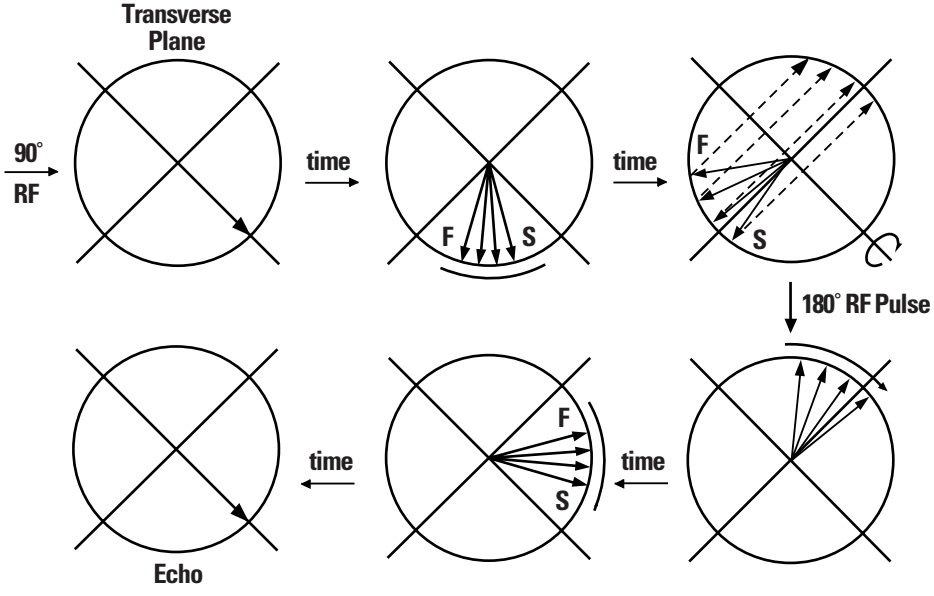

FIGURE 11 – Mechanism of spin echo magnetization which begins to lose phase coherence largely due to B_0 inhomogeneity. As the magnetization precesses and fans out in the transverse plane, the fast (F) and slow (S) edges of the magnetization can be identified. The 180° pulse rotates all of the magnetization up out of the transverse plane and back down onto the opposite side of the transverse plane. Precession now continues in the same direction as before, but now the fast edge is behind the slow edge leading to re-phasing and echo formation.

BACK

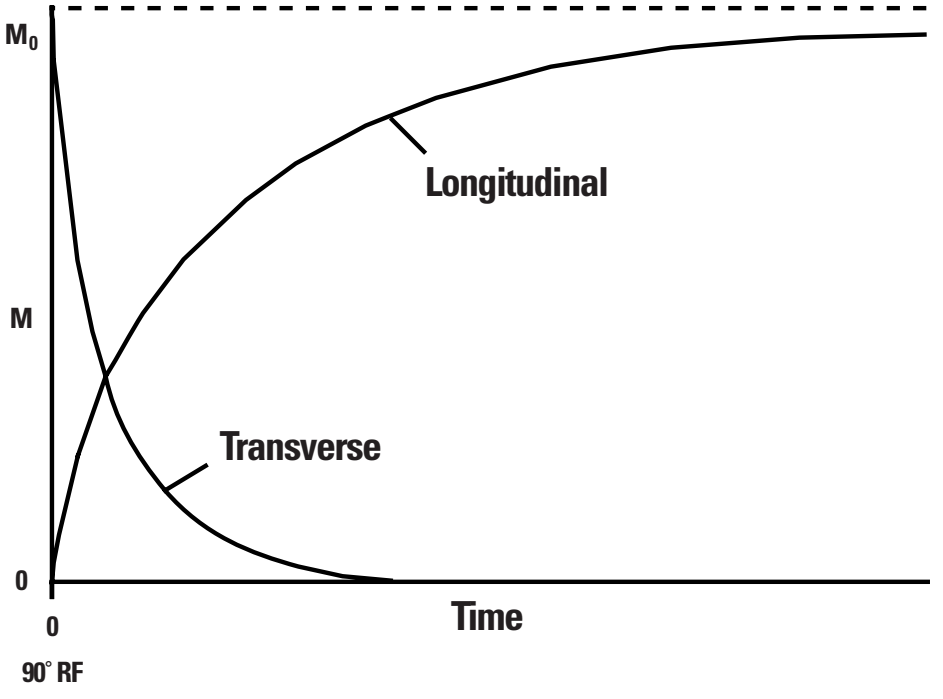

FIGURE 12 – After a 90° RF pulse, all of the magnetization lies in the transverse plane. T2 processes and B_0 inhomogeneity lead to an exponential decay of transverse magnetization, while longitudinal magnetization increases with time.

BACK

Longitudinal relaxation restores the original equilibrium population difference by returning some spins to the lower energy state, and in the process giving up energy to the environment (lattice).

Longitudinal relaxation seems to share some of the features observed for transverse relaxation; both are characterized by exponential evolution. In what may be viewed as complementary processes, transverse magnetization decays, from maximum to zero, while longitudinal magnetization builds up from zero to maximum. Not surprisingly then, the quantitative expression for T1 relaxation looks similar to what was seen for T2:

$$[3] \quad M_{longitudinal} = M^0_{longitudinal} (1 - e^{-t/T1})$$

Equation [3] predicts the amount of longitudinal magnetization that will be present at time = **t** ($M_{longitudinal}$) and the value of **T1**. **T1** is the length of time necessary to decrease the difference between the current value of $M_{longitudinal}$ and the equilibrium value by a factor of **(1 – 1/e) = (1 – 1/2.7) = 63%**. This statement implies that the rate of increase in longitudinal magnetization is fastest when $M_{longitudinal}$ is very different from its equilibrium value. In (**FIG. 12**), this concept of a decreasing rate of change over time is seen graphically. Comparing T1 and T2 for any given system, T1 is always greater than or equal to T2.

Factors Influencing Relaxation Rates

What physical factors affect the observed relaxation times? In general, the same conditions that shorten (or lengthen) T1 also shorten (or lengthen) T2. There may be more than one mechanism acting to yield T1 and/or T2 relaxation, in which case the observed relaxation (T1 or T2) due to the combined action of mechanisms labeled generically as "a, b, c . . ." is given by:

$$[4] \quad \frac{1}{T\,observe} = \frac{1}{Ta} + \frac{1}{Tb} + \frac{1}{Tc} + \cdots$$

Due to this sum of reciprocals relationship, the longer the relaxation time, the greater the change caused by the introduction of an additional mechanism on the observed relaxation time.

CONTINUED

For pure water T1 = T2, whereas in tissues T1 >> T2. The total range over which T2 can change in pathological situations is therefore much greater. In fact, in edema, for example, T2 may be prolonged several hundred percent. It is for this reason that images highlighting variations of T2 are most sensitive in detecting pathology (**REF. 11**). (**TABLE 2**) gives T1 and T2 values encountered in various normal tissues.

The rate of relaxation is strongly influenced by the rate at which the molecules bearing the protons being observed tumble in solution. Slower tumbling yields faster relaxation (shorter relaxation times). When tumbling is very slow, as in the case of protons covalently bound to macromolecules (proteins, nucleic acids, etc.), T2 is so short that their signals decay completely between excitation and detection.

In MRI, only "mobile" protons can contribute signals for imaging These mobile protons are in the form of water and some lipids. Since lipid molecules are larger than water molecules, and hence tumble more slowly, in general, lipid protons relax more quickly than water protons.

The issue of water relaxation *in vivo* is complicated by the fact that water molecules spend part of the time freely tumbling while surrounded by other water molecules, and part of the time loosely bound to the surface of macromolecules. Because there is a very rapid exchange between this "free" and "bound" water, this leads to an observation of relaxation times which reflect an average of relaxation as bound and free water. Thus, the greater the percentage of the time that an average water molecule is in a bound state, the shorter the relaxation time.

Consider what parameters influence this ratio of time spent in free and bound states. Certainly the percent of water in a given tissue would have an effect. Indeed, tissues with lower water content display shorter relaxation times than tissues possessing higher water concentrations. The chemical nature of the tissue may also have a role in the determination of this free/bound ratio.

CONTINUED

Tissue	T1	T2
White matter	390	90
Gray matter	520	100
Cerebrospinal fluid	2000	300
Skeletal muscle	600	40
Fat	180	90
Liver	270	50
Renal medula	680	140
Renal cortex	360	70
Blood	800	180

TABLE 2 – Representative relaxation times for various tissues[1]

1 Appropriate values in milliseconds measured at 1.0 Tesla (REF. 10)

BACK

For a tissue like the white matter of the brain containing a great amount of high molecular weight lipids (myelin), water spends less time in a bound state than it might otherwise—simply because oil and water do not mix.

The strength of the B_0 field also influences relaxation times. This is due to the fact that the efficiency of relaxation is related to the ratio of the tumbling rate to the reciprocal of the Larmor frequency. In general, T1 relaxation times are shorter at lower field strengths. The presence of paramagnetic species such as iron and paramagnetic contrast agents (e.g. Gd + 3 DTPA) will shorten relaxation times. Their effect is first observed on T1 and then with increasing paramagnetic concentrations, on T2 as well. For more information on basic spin physics of relaxation, the reader is directed to (**REFS. 1–4**) in the Bibliography.

The Effect of Magnetic Field Gradients

In a broad sense, a magnetic field gradient simply refers to the spatial variation of the strength of the B_0 field. This was encountered previously when discussing the dephasing effects of B_0 inhomogeneity, which may be viewed as an irregular spatial variation of B_0. For the purposes of imaging however, field gradients like those illustrated in (**FIG. 13**) are needed. The slope of the gradient, its direction (i.e. along what axis), and timing need to be controlled. Furthermore, for most applications, the B_0 field must be caused to vary in a linear fashion with distance. Note that a gradient does not change the direction of B_0 but rather it changes the spatial variation of the amplitude of the B_0 field.

CONTINUED

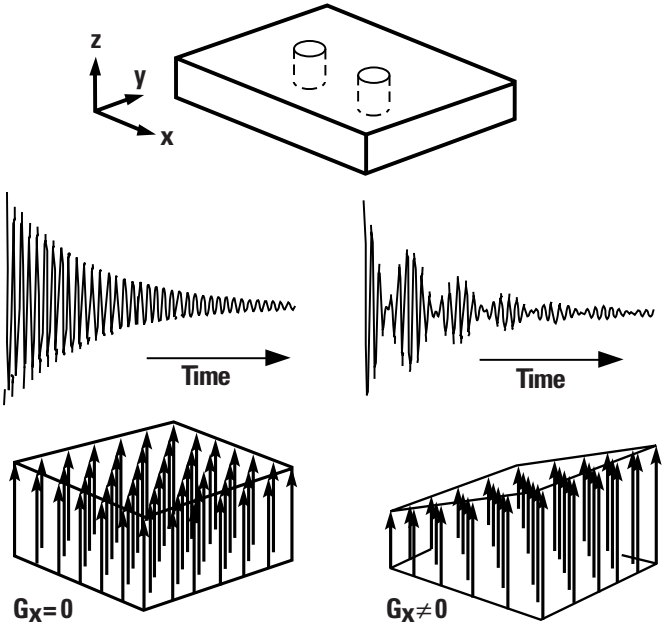

FIGURE 13 – The object at the top of the figure contains two small waterfilled cylinders. (A) In the absence of a gradient, the B_0 field is the same at all points in the object as depicted by the set of vectors. Application of an RF pulse to the object yields a FID consisting of a single frequency. (B) Here, a gradient of the B_0 field is imposed along the x-axis of the object. The spins in the two cylinders are exposed to different B_0 fields and thus possess different Larmor frequencies. An RF pulse now gives an FID which is an interference pattern of the two frequencies.

BACK

Suppose that there exists a linear gradient along one spatial axis. Since

$$\gamma B_0 = F \quad [1]$$

the resonance (Larmor) frequencies of protons will vary according to their positions along the gradient axis. This is key to the understanding of image formation. Since we can measure frequencies and we know the imposed spatial variation of B_0, the positions of resonating protons can be determined from their frequencies.

In summary, a magnetic field gradient causes transverse magnetization to precess at a frequency which is proportional to position along the gradient axis as follows:

$$F = \gamma (B_0 + r G_r) \quad [5]$$

Where r is position along the axis of the gradient G_r. The presence of a gradient has no significant effect on longitudinal magnetization.

Let us now consider the fate of transverse magnetization when a gradient is switched on for a short period of time and then switched off (**FIG. 14**). It may seem odd at first, but transverse magnetization can "remember" the effect of gradients which were present at an earlier time. Following RF excitation and before imposition of the gradient, transverse magnetization arising from three different positions along the gradient axis, are all precessing together (in phase) at the same frequency. When the gradient is turned on, the vectors rotate at different rates (frequencies) according to position. When the gradient is turned off, all of the precessional frequencies are again the same, but the vectors representing transverse magnetization are no longer in phase. Continued precession, all at the same frequency, will not change the angles (relative phases) between the three vectors. The action of the past gradient pulse is thus remembered as "phase memory" (**REF. 5**).

CONTINUED

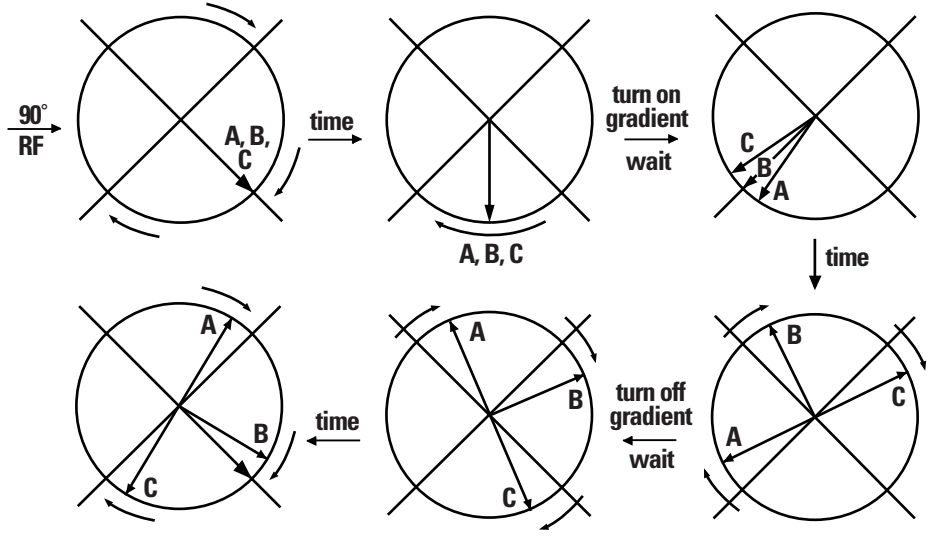

FIGURE 14 – Phase memory. Spins at three distinct locations (A,B,C) along a gradient axis is shown. A 90° RF pulse generates transverse magnetization from all three sites. In the absence of a gradient, vectors A,B,C precess in phase. When the gradient is switched on, the spins at locations A,B and C are exposed to different B_0 fields, which in turn give rise to different precessional frequencies for the three locations. While the gradient remains on, the relative phase angles, e.g. between vectors A and B or B and C, become larger and larger. However, when the gradient is switched off the precessional rates for A, B, and C become equal again. Continued precession does not alter the phase (angular) relationships between the three vectors.

BACK

Fourier Transformation

We have seen that the basis for image formation is a positionally dependent frequency response of transverse magnetization. Thus, an image is a graph of amplitude versus frequency (**FIG. 15**). There remains a problem, however. The signals that are received, like the FID in (**FIG. 8**) or the echo in (**FIG. 10**) are in the form of amplitude versus time, rather than amplitude versus frequency, as needed for an image. At first this may seem to be a trivial problem. Looking at the FID in (**FIG. 8**), the frequency of the signal is easily determined as the reciprocal of the time interval between two adjacent peaks. What makes the problem less than trivial is that signals are received from all positions *at the same time.* The resultant signal is the superimposition (or sum) of a multitude of frequency components, each with distinct amplitudes and relative phases. Thus, it is an interference pattern composed of all these components. A procedure is needed which can determine what set of frequencies, amplitudes and phases would give rise to the observed interference pattern. Such a procedure would be called a transformation from the time domain to the frequency domain.

Most MR imaging and NMR spectroscopy makes use of the Fourier transform (FT), named after J.B.J. Fourier (1768-1830) who developed the mathematical theory. In 1960, researchers at IBM devised a new algorithm for calculating the Fourier transform of arbitrarily complex digitized waveforms. The new algorithm (the Fast Fourier transform or FFT) greatly reduced the number of arithmetic operations necessary to calculate Fourier transforms. Although the required number of operations is still quite large, fast computers can accomplish an FFT in a fraction of a second. (**REF. 17**)

A sinusoidal waveform (a sine wave) is completely defined by specifying three quantities: the amplitude, the period (or its reciprocal frequency) and the phase. The phase of a sinusoid describes what point in the wave cycle the sinusoid displays a given time versus a reference sinusoid of the same frequency.

CONTINUED

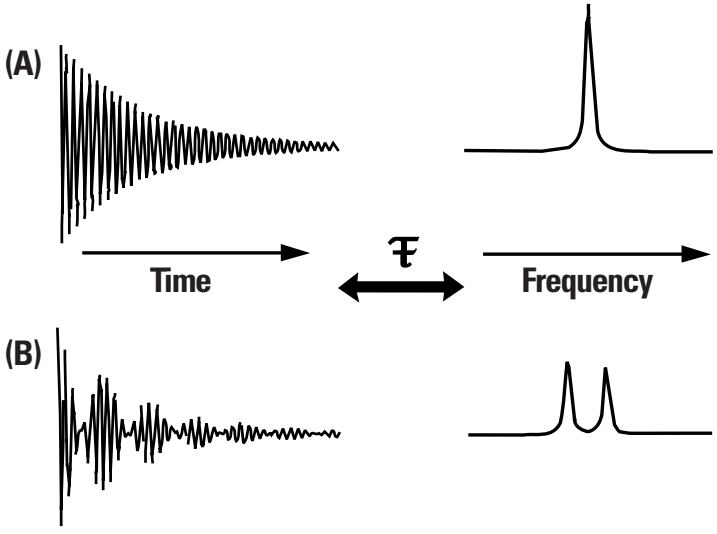

FIGURE 15 – (A) The Fourier transform is a mathematical process which mediates the interconversion of time (units of sec.) and frequency (units of 1/sec. = Hz) descriptions of waveforms. If two adjacent peaks in FID "A" are found to be separated by 0.01 see, the FT will yield a peak at 1/0.01 sec., = 100 Hz. (B) The power of the FT is its ability to sort out arbitrarily complex time domain waveforms into their individual frequency components The time domain signal here is an interference pattern which arose due to imposition of a gradient across the object in FIGURE 13. The FT shows the two component frequencies. Since the gradient causes variation of frequency with distance, the frequency domain here represents a one-dimensional projection image of the object.

BACK

This is the same as the description of the relationship between the three vectors in the last section after turning off the gradient. Fourier transformation conserves all three pieces of information. In clinical MR imaging, however, the phase information is usually discarded at the final stage of reconstruction.

Frequency is the reciprocal of time, and time is the reciprocal of frequency; the FT of the time domain is the frequency domain, and vice versa. The information content in the two domains is identical, but the format is different.

The necessity of examining information in one domain instead of the other actually arises from the constraints of human perception. (*For an example, see the Reconstruction section under MR Imaging Techniques.*) We are capable of something like a mental FT when we listen to a chord of music. The sound arrives at our ears as an interference pattern of the notes of the chord; however, we can still discern individual notes played together to yield that chord (**REFS. 4, 18**). By contrast, the eye is not capable of extracting individual wavelengths of, say, white light. This decomposition, however, can be achieved by means of a prism which serves as a Fourier analyzer.

CONTINUED

CHAPTER 2

Principles and Techniques in MR Imaging

Instrumentation

From the preceding discussion, the equipment necessary for MR imaging can largely be inferred. A typical MR imaging system block diagram is given in (**FIG. 16**).

The B_0 Field

The source of the static B_0 magnetic field is a magnet large enough for a person to be positioned in its homogeneous portion. The property of prime importance is the strength of B_0. High magnetic field strengths are desirable because, as discussed on pages 72-78, this parameter ultimately limits the strength of the MR signals to be received. High magnetic field strengths require a superconducting magnet such as that diagramed in (**FIG. 17**).

Beyond the nominal strength of the B_0 field, the homogeneity of this field over the imaging volume must be considered. B_0 inhomogeneity of just a few parts per million (ppm) leads to noticeable shading of MR images, while greater inhomogeneities give rise to spatial distortions in the images.

Clearly, much of the advantage of high-field strength can be lost without sufficient homogeneity. B_0 homogeneity is optimized by a procedure known as "shimming". Here, the magnet is fitted with a set of electromagnetic coils. By carefully adjusting the amount of current in each of these coils, the B_0 field over the imaging volume is adjusted or shaped until acceptable homogeneity is achieved.

CONTINUED

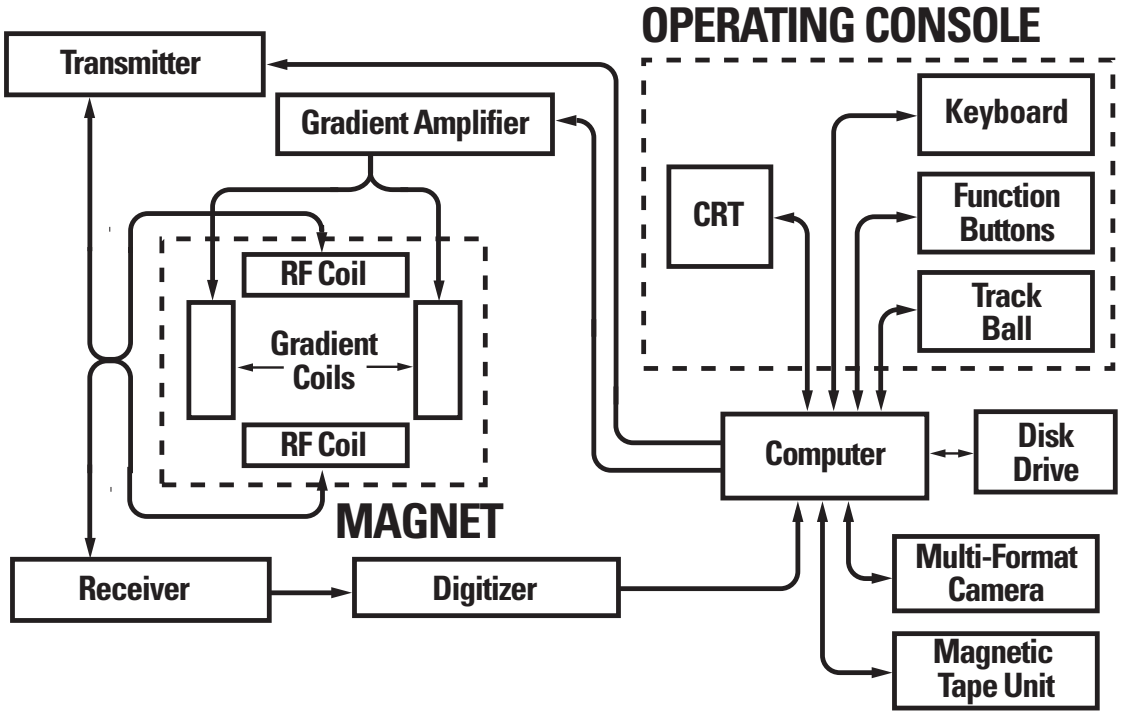

FIGURE 16 – Functional block diagram of an MR imaging system.

BACK

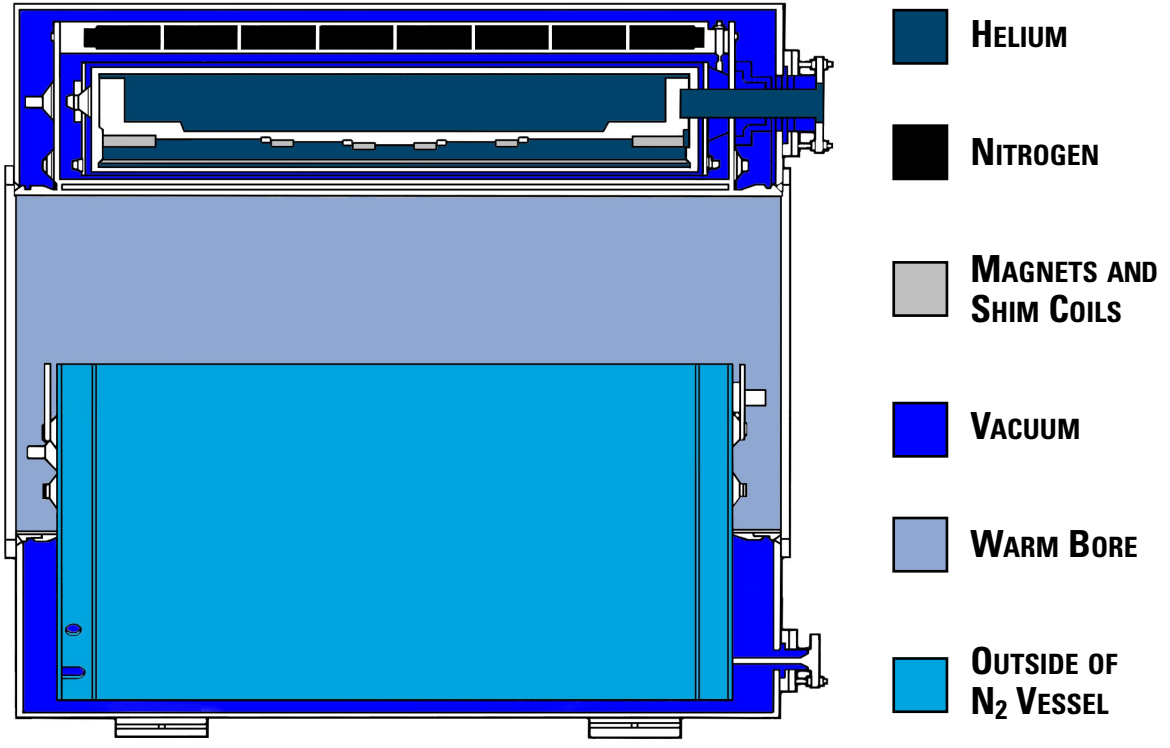

FIGURE 17 – Cross-sectional view of superconducting magnet.

BACK

Magnetic Field Gradients

As discussed earlier, gradients in the B_0 field along the three orthogonal spatial axes are fundamental to image production. Gradients along other oblique axes can be implemented with combinations of the orthogonal gradients.

(**FIG. 18**) shows the basic scheme for obtaining a B_0 gradient parallel to the direction of B_0. Two coils of wire (a), and (b), are supplied current which generates magnetic fields, adding (a) or subtracting (b) from the main B_0 field. At any given point along the gradient axis, the net magnetic field is equal to the sum of B_0 plus the magnetic field contribution from coil (a) plus the contribution from coil (b). It is the coil which is closer to the position of interest that has the greater effect on the net magnetic field.

Note that at a point midway between the two coils, the magnetic fields generated by the two gradient coils cancel each other, causing the net magnetic field to be equal to B_0. The gradient coils are positioned such that this mid-point is at the center of the B_0 magnet, and is denoted as the isocenter.

The gradient coils on the other two orthogonal axes are constructed differently, but they also cause additions and subtractions to the B_0 field dependent upon position alone these axes. Additionally, the mid-points of no net gradient contributions are positioned to occur at the magnet's isocenter. Power is supplied to each of the gradient coils by independent computer-controlled gradient amplifier.

What properties of the magnetic field gradients impact upon system performance and ultimately image quality? There are several. As shown in the next three sections, the maximum attainable gradient amplitude (or slope, which is the change in magnetic field per unit distance, often cited in terms of Gauss/cm) limits the minimum slice thickness and the minimum field-of-view (FOV) that can be used. Gradient linearity refers to the uniformity of the slope along the gradient axis; non-linearity yields image distortions.

CONTINUED

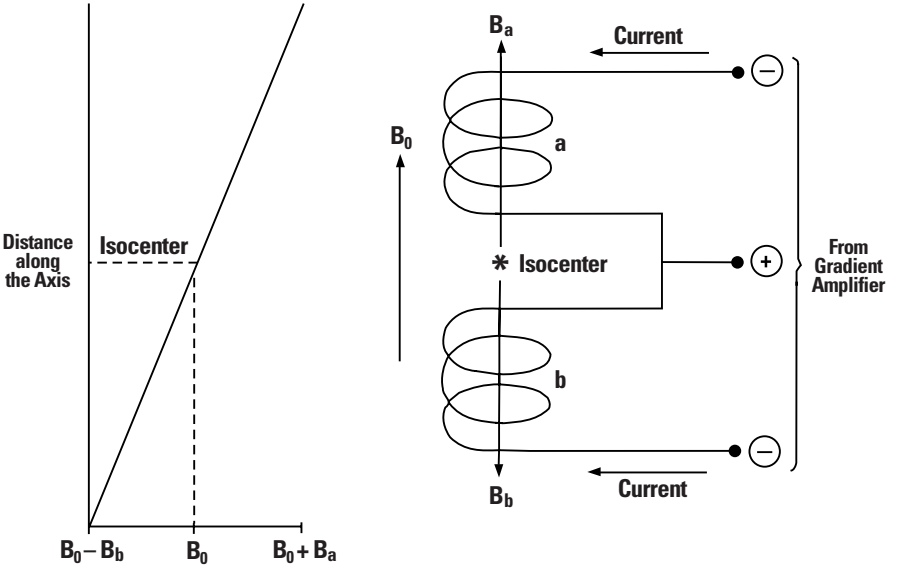

FIGURE 18 – The design of a gradient coil acting parallel to B_0. The coil is divided into two sections (a and b) which are supplied DC current from the gradient amplifier for this axis. Coil "a" produces a magnetic field B_a which adds to B_0, while coil "b" produces B_b subtracting from B_0. The strength of B_a and B_b. decreases with increasing distance from coils "a" and "b" respectively, while the strength of B_0 is constant over this region. At any point along this axis the net magnetic field (B_{net}) is the sum of B_0, B_a, and B_b. This results in a linear variation of B_{net}; B_a and B_b cancel at isocenter giving B_{net}, = B_0 at that position.

BACK

In practice, gradients are not powered at all times, but are switched on and then off again (pulsed) at certain times during a pulse sequence. This raises further concerns. How fast a gradient can be powered from zero to full amplitude is referred to as the "rise time," which should be as short as possible.

But the act of switching gradients on and off causes another problem. It induces the formation of electronic currents, so-called "eddy currents" in the metallic structures of the magnet. These eddy currents generate magnetic fields of their own, which dissipate at differing rates. Clearly, eddy currents are undesirable and can have deleterious effects on image quality.

One solution to this problem is to drive the gradient coils not with the desired pulse shape, but rather with an empirically determined pulse shape which cancels out eddy current contributions and yields the desired gradient in the magnet.

A potentially more powerful approach is the use of self-shielded gradient coils. These coils are constructed such that the magnetic fields generated by them are confined to the interior of the coils thus preventing the formation of eddy currents in the remainder of the magnet.

The B_1 Field

The basic RF architecture for generation of RF pulses constituting the B_1 field is diagramed in (**FIG. 19**). An extremely precise and stable source of RF at low power levels is a digital frequency synthesizer set to yield RF at the proton Larmor frequency (F_0) in the absence of gradient contributions. As discussed under slice selective excitation (*Last Section*), it is useful to be able to make small changes (ΔF_0) to the value of F_0; waveform modulation and pulse control are also essential. An RF power amplifier then varies the RF power to that required for imaging. All of these stages are controlled by a computer, which is also responsible for pulse sequence execution. The final RF energy is sent to the RF coil in the magnet which acts as a broadcasting antenna.

CONTINUED

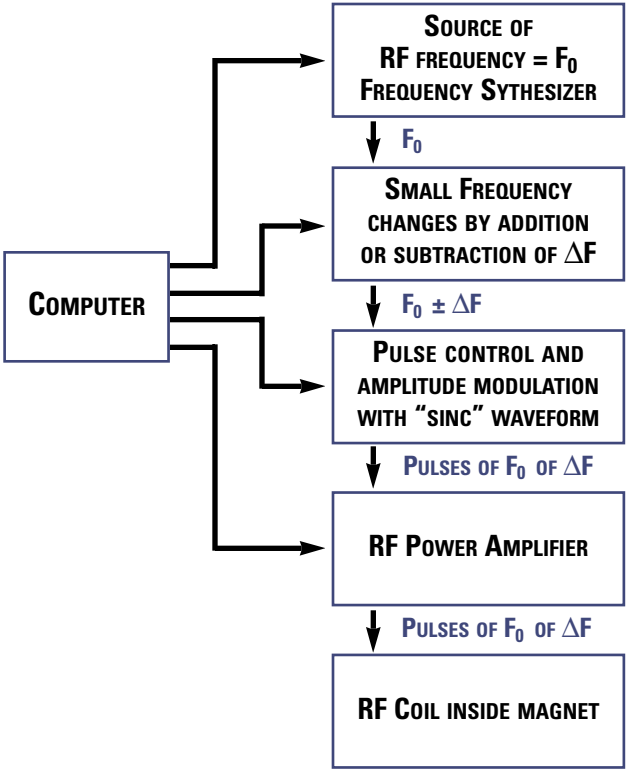

FIGURE 19 – Functional block diagram of the RF transmitter section of an MR instrument. A digital frequency synthesizer with a thermostated quartz crystal reference produces low amplitude RF of frequency F_0 which is the Larmor frequency at B_0. Slice selective excitation requires the ability to make small frequency changes to F_0, which is accomplished by addition or subtraction of an "offset" frequency (ΔF_0). Waveform modulation serves to control the profile of the excited slice, and pulse control determines when RF is allowed to pass to the final RF power amplifier.

BACK

For most applications, it is desirable for the RF coil to distribute the RF energy uniformly throughout the imaging volume. The degree to which this is achieved depends primarily on the design of the RF coil. Critical Performance specifications include the maximum amount of power that the RF power amplifier is capable of producing.

Remember, the flip angle is proportional to both the duration and the amplitude of the RF pulse. Furthermore, the linearity of this amplifier is critical. A linear amplifier is one in which a change in the amplitude of the input signal leads to a directly proportional change in the amplitude of the output signal. RF amplifier non-linearities yield flip angle errors as well as distortion of the shape of an excited slice.

The Receiver

The task of the MR receiver can be appreciated when it is realized that the signal resulting from nuclear transverse magnetization is approximately one billionth that of the transmitted RF power. A simplified design of an MR receiver is given in (**FIG. 20**).

Transverse magnetization induces an AC current in the RF coil used for reception; this coil may or may not be the same RF coil used for production of the B_1 field. The RF signal, which is approximately at the Larmor frequency for the B_0 field is amplified by a factor of 10^4 to 10^5 by the RF preamplifier. It is technically quite inconvenient to work at these high frequencies. The ultimate function of the receiver is to correctly represent the amplitude, periodicity and the phase of the incoming MR signal in computer memory. For this purpose, it is only necessary to measure the MR signal relative to a known standard.

The standard used is a RF source called the local oscillator, which in fact is often a portion of the RF signal from the frequency synthesizer used for transmission. The mixer then yields a signal which is the difference between the RF transmitted and the signal received. This difference signal is in the range of audio frequencies (AF). It is this range of frequencies which are of concern for the receiver bandwidth.

CONTINUED

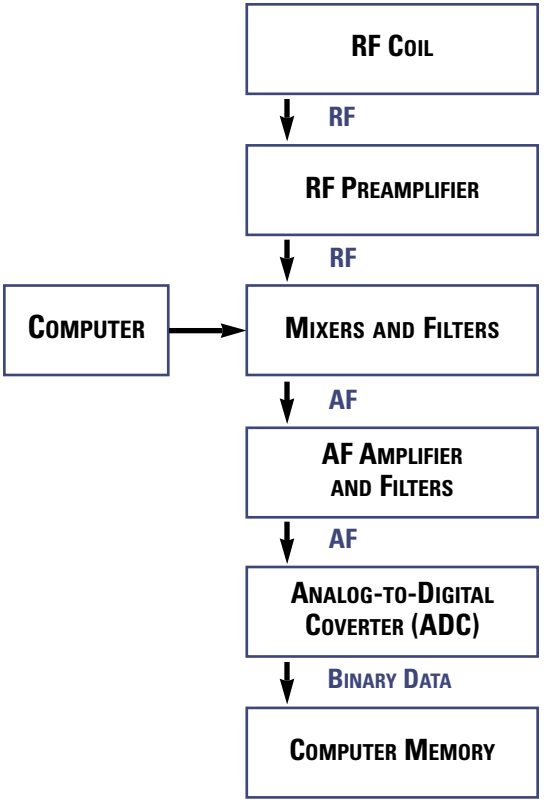

FIGURE 20 – Block diagram of an MR receiver. Transverse magnetization induces an AC current in the RF coil which is amplified. This signal is mixed with a reference RF signal from the "local oscillator;" this oscillator may actually be the frequency synthesizer used for RF transmission in FIGURE 19 (not true for off-center FOV). The low frequency (AF) signal which is the difference between the incoming RF and the local oscillator RF is then amplified, digitized and stored in computer memory.

BACK

The AF signal is amplified by a factor of 10 to 1,000 by an AF amplifier. The signal is next directed to an analog- to-digital converter which converts the AF signal into a series of binary numbers. These numbers are then stored in computer memory for later manipulation (signal averaging and Fourier transformation).

The most critical design feature of the receiver is the combination of the quality of the RF coil and RF preamplifier. These two components predominantly determine the amount of system noise added to the MR signal. Of somewhat lesser importance for imaging is the precision of the ADC; 12-bit resolution is usually sufficient for imaging.

The Computer System

A modern MR instrument imager has several computers linked by a communications network. For example, the current Signa® system has four computers: a host computer, an array processor, and two specialized computers which are the status control module (SCM) and the pulse control module (PCM). It is not necessary to have this particular partitioning of computing power. Therefore, the features of a MR computer system as a whole will be discussed here.

Core memory is directly accessed by the central processing unit(s) (CPU). This memory must be sufficiently large to contain all of the instructions and waveforms for one pulse sequence, an entire raw image data set, and a certain amount of operating software. The remaining software and data requirements can be met with disk memory.

An array processor is needed in order to accomplish image reconstruction quickly. This implies that the array processor requires direct access to at least enough memory to carry-out reconstruction of an entire image, otherwise disk access operation becomes rate-limiting. Since pulse sequences must execute in “real time,, the computer system must give top priority to pulse sequence instruction execution. The receiver ADC must have buffered memory access to ensure that incoming data can be stored quickly enough that data are not missed or lost.

CONTINUED

Long-term data storage (archiving) is generally relegated to streaming tape.

The computer system described here is a minimal configuration. In actual practice, more powerful systems are employed in order to ease prescriptions and routine operations.

In the following discussion of the image acquisition process, we will concentrate on the most commonly implemented clinical technique, i.e. two-dimensional Fourier transform imaging utilizing spin-warp encoded spin echoes. (**REFS. 5–8, 23**).

Slice Selective Excitation

In 2D-imaging schemes, signal response in the third spatial dimension needs to be restricted. This is accomplished by selectively exciting (converting longitudinal magnetization into transverse magnetization) only spins in a well defined slice of tissue within the imaging volume. This is accomplished by imposing a gradient on an axis perpendicular to the chosen slice plane, which causes a linear variation of potential resonance frequencies along that axis (**FIG. 21**). Input of RF energy consisting of a narrow range of frequencies (RF bandwidth denoted as ΔF) excites only those spins along the slice selection axis whose resonance frequencies, as dictated by the gradient, correspond to the frequencies present in the RF. After the RF pulse, the slice selection gradient is turned off, and signals emanating from the chosen slice can be detected.

Quantitatively, the thickness of the excited slice ($\mathbf{d_{sl}}$) in cm is related to the gradient amplitude G_{slice} and RF bandwidth ΔF as follows:

$$\Delta F = \gamma_H * G_{sl} * d_{sl} \quad [6]$$

For example, suppose that without any gradient all protons resonate at 64.000 MHz and that the RF covers the range 64.001 MHz to 63.999 MHz. The RF bandwidth (ΔF) is 0.002 MHz 2000 Hz. If a gradient amplitude of 0.5 Gauss/cm is imposed and the RF pulse is issued, the thickness of the excited slice is:

$$\frac{2000 \text{ Hz}}{4257 \text{ Hz/Gauss} \times 0.5 \text{ Gauss/cm}} = 0.94 \text{ cm}$$

CONTINUED

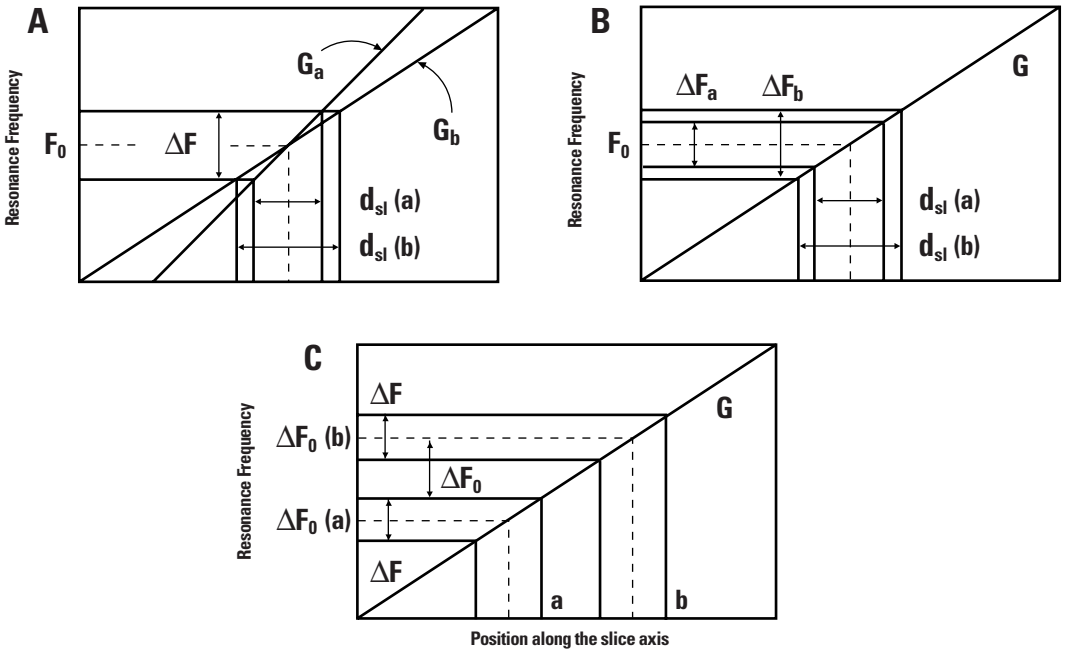

FIGURE 21 – Slice selective excitation is accomplished by the use of narrow bandwidth (ΔF) RF in combination with a gradient along the slice axis. A and B show two possible strategies for variation of slice thickness. In A the gradient amplitude is varied, while in B the gradient amplitude is constant but ΔF is changed. In C, different slice locations are chosen by changing the RF center frequency (F_0).

BACK

If a thinner slice is desired, two options become evident from Equation [6]: either (a) the RF bandwidth must be decreased or (b) the gradient amplitude must be increased.

Let's assume a single slice has been excited. But which slice? And at which location along the gradient axis? As noted in the previous section, the gradient coils are constructed such that the zero point of the gradient is a magnetic center (the isocenter) of the magnet. This means that for any of the three gradients at any amplitude, B_0 at isocenter is unchanged. Along a given axis, the gradient causes a linear increase of B_0 on one side of isocenter, and a linear decrease of B_0 with increasing distance from the other side of isocenter.

Now, the location of the excited slice can be determined. Since the center frequency of the RF (F_0) was equal to the resonance frequency of protons in the absence of a gradient, and since at isocenter there is no change to B_0 when a gradient is on, the slice excited above was located at isocenter + 0.47 cm.

This, however, raises yet another question. How can one selectively excite an off-isocenter slice? Again there are two options: (a) change the position of the zero point of the slice selection gradient with respect to isocenter, or (b) change the center frequency of the RF to correspond to a resonance frequency which is either higher or lower than the proton resonance frequency without gradients. Practical considerations force the choice of the latter option. This method of offsetting a slice from isocenter is also easy to examine quantitatively. If the same slice thickness, gradient amplitude and bandwidth (ΔF) as in the above example are employed, then the needed change for the RF center frequency (ΔF_0) is expressed by:

$$\Delta F_0 = \frac{\text{OFFSET} * F}{d_{sl}} \quad [7]$$

where offset is the distance from isocenter for the center of the desired slice.

CONTINUED

For example, if the desired slice location is +3.76 cm from iso-center then the center RF frequency is changed by:

$$\Delta F_0 = \frac{3.76 \text{ cm} \times 2000 \text{ Hz}}{0.94 \text{ cm}} = +8000 \text{ Hz}$$

Now the RF covers the range 64.009 MHz to 64.007 MHz.

There is one more issue in the slice selection process that merits discussion.

If one could examine the excited slice and its profile edge-on, how would it appear? One might hope that the slice profile would be rectangular; however, without special precautions this would not be the case. It is necessary to insure that the flip angle is uniform across the slice If RF at frequency = F_0 is just switched on for some period of time and then switched off, the flip angle will not be the same at all depths in the slice (**FIG. 22**). The nonuniformity of flip angle across the slice is a consequence of the variation in RF amplitude at different frequencies (depths in the slice). We now see that earlier statements concerning RF covering a range of frequencies bore a rather stringent implied assumption: there is an equal amount of RF power input for all frequencies within F, and no power outside of this range.

The FT can point to the solution of this problem. Note that in (**FIG. 22A**), the rectangular pulse of RF is a description of amplitude versus time, while its corresponding plot of RF power distribution is amplitude versus frequency. This should sound familiar. Indeed the FT of a rectangular pulse envelope is this curve defined by the function sin x/x called a "sinc" waveform. Due to the aforementioned reciprocity between the time and frequency domains, the solution suggested is as depicted in (**FIG. 22B**). If a rectangular frequency domain profile is desired, then the FT of a rectangle, namely the sinc shape is the needed time domain description of the RF pulse. In practice then, the RF pulse of frequency = F_0 is multiplied by the sinc waveform before sending the pulse to the RF coil in the magnet. We have seen how to confine excitation to a single slice in the imaging volume.

CONTINUED

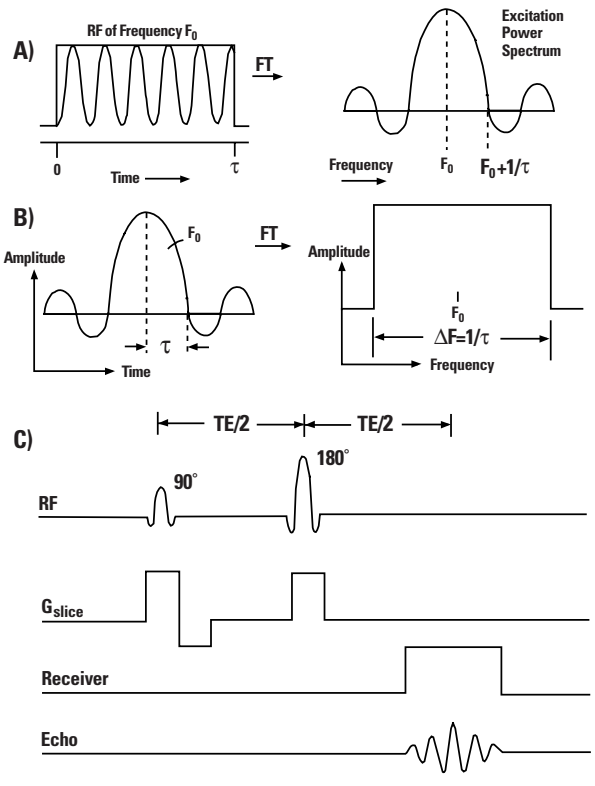

FIGURE 22 – (A) Although the reasons are not intuitively obvious, a short burst or pulse of single frequency RF does not result in deposition of RF power at just one frequency. Instead, the RF power is spread over a range of frequencies centered at F_0. If such a pulse of RF were used for slice selection, the variation of RF power across the resonance frequencies contained in the slice would yield variations in flip angle across the slice. (B) This situation is avoided by using a "sinc" shaped RF pulse to give a rectangular RF power spectrum. (C) Sinc pulses are incorporated into a slice selective spin echo sequence. Note the standard schematic representation of gradient action. The height of a gradient pulse represents the amplitude or slope of the gradient, and the width its duration. Whether the gradient causes increasing or decreasing B_0 when moving in a positive direction along the gradient axis is indicated by a pulse up or down. The small negative-going lobe of G_{slice} accounts for dephasing which occurs during the slice selective 90° pulse.

BACK

In fact, since spin-echoes are to be used, two selective RF pulses, a 90° pulse and a 180° pulse, are employed to obtain a slice selective spin-echo.

Frequency Encoding

The next task is encoding the image information within the excited slice. The image information sought is actually the amplitude of the MR signal arising from the various locations in the slice. Two distinct processes are used for encoding the two dimensions, called frequency encoding and phase encoding. Frequency encoding will be discussed first.

The general strategy for gaining spatial information along one axis of the image plane is shown schematically in (FIG. 23A). For reasons of sensitivity, it is desirable to have the receiver on only while the echo is present, and to have the center of the echo form in the middle of this "acquisition window". This action, in combination with slice selection, would not yield information about distribution of spins within the slice, because all positions would resonate at the same frequency. Imposition of a gradient along one of the two principal axes of the plane during the period when the receiver is on, causes the signal received to be an interference pattern arising from the various precessional frequencies of the spins along the gradient axis, hence the name frequency encoding This gradient is sometimes referred to as the "read", "read-out", or "frequency-encoding" gradient. The FT of the signal acquired in the presence of the read gradient is an image of the projection of the slice onto the read gradient axis. (FIG. 13) & (FIG. 15)

If only the read gradient pulse were played on this axis, severe dephasing of the echo and concomitant loss of signal intensity would be anticipated. In order to avoid this, another gradient pulse, termed a "dephaser", is also implemented along the frequency encoding axis. Note that the area of the dephaser gradient pulse is one half that of the read gradient. The dephaser changes the phase of transverse magnetization by amounts which are proportional to position along this axis (FIG. 23B).

CONTINUED

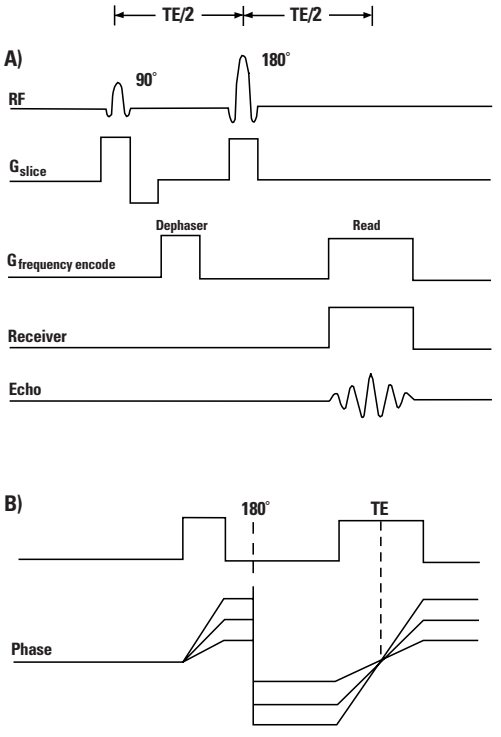

FIGURE 23 – Frequency encoding. (A) The frequency encoding gradient is played along one of the two principal axes with the selected slice. The read gradient pulse causes the frequencies contained within the spin echo to be proportional to the positions of responding spins along the axis of the frequency encoding gradient. In order to avoid severe dephasing of the echo due to the read gradient, a "dephaser" of pulse is used. (b) Instead of representing phases by the direction of vectors in a circle in the transverse plane, a useful convention is a phase plot where the circle is represented on an axis running from + 180° to -180°. The dephaser causes a positionally dependent phase change as shown for three positions (FIGURE 14). The 180° pulse reverses these phases, and the first half of the read gradient causes rephasing; all positions are in phase at echo time.

BACK

The 180° pulse inverts this phase distribution, just as it did in the discussion of spin-echo formation. The action of the first half of the gradient over the acquisition window now acts to compensate the phase shift caused by the first gradient pulse on this axis. In this manner, complete rephasing occurs at time TE, i.e. in the center of the acquisition window.

The details of the frequency encoding procedure dictate the field of view along this axis: (**FOV_f**).

[8] $$\gamma G_f \bullet FOV_f = BW$$

Where **G_f** is the amplitude of the frequency-encoding gradient, and **BW** is the receiver bandwidth. Note that Equation **[8]** is directly derived from the Larmor equation. The receiver bandwidth should not be confused with the RF bandwidth discussed in the previous section, although the relationships between the various quantities are closely analogous in the two situations.

In order to gain an understanding of receiver bandwidth and its role in determining the FOV, it is necessary to review the action of the MR receiver, and examine the details of signal digitization.

Within the receiver, the incoming RF signal is converted to a much lower (AF) frequency which is the difference between the RF transmitted and that received. This difference signal is digitized by sampling the voltage of the signal at discrete intervals and then representing these voltages as digital numbers to be used by the computer (**FIG. 24**). Sampling theory dictates that in order to gain a correct digital representation of the frequency of a sinusoidal waveform, it is necessary to sample the waveform at least twice per cycle.

Thus, it is the rate at which the signal is sampled which determines the maximum interpretable frequency in the signal. This maximum frequency is called the Nyquist frequency. Frequencies present in the signal which are higher than the Nyquist frequency will be misrepresented in digital form, and will appear to be contributions which are lower than the Nyquist frequency. This is the cause of “wrap-around” artifacts.

CONTINUED

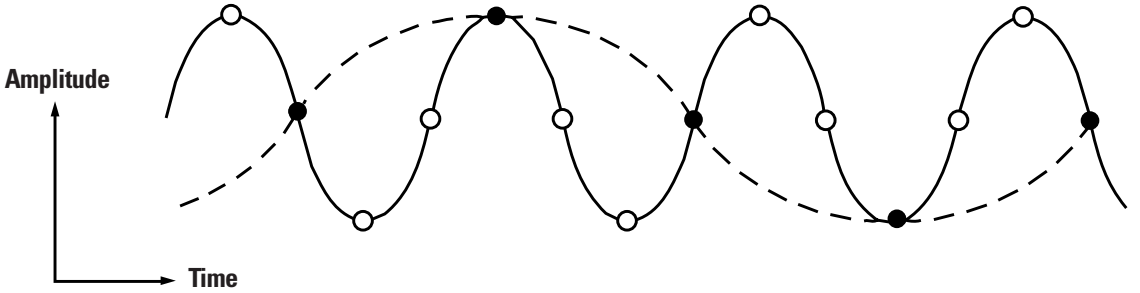

FIGURE 24 – A sine wave (solid line) is "sampled" at the times of the open circles and the amplitudes at those times are digitized for computer storage. However, if the sine wave is not sampled at least twice per cycle (closed circles), the computer representation of the sine wave gives an erroneous impression of the wave's frequency.

The effective range of frequencies that can be properly detected (receiver bandwidth) is controlled by the digital sampling rate, which in turn is determined by the number of points on the signal to be digitized and the length of time that the receiver is on. Therefore:

$$[9] \qquad BW = N_f / T$$

Where N_f is the number of complex points* sampled, and T is the sampling time.

As an example, let us examine the default values implemented on the Signa system. All available matrix sizes use 256 complex points in the frequency encoding dimension, and acquisition window duration 8 msec. The receiver bandwidth is:

$$BW = \frac{256/.008 = 32.000 \text{ Hz} = \pm 16 \text{ kHz})^*}{2 \times 0.008 \text{ sec}}$$

The FOV_f is adjusted through variation of the amplitude of the read gradient (G_f). If G_f= 05 Gauss/cm, then:

$$FOV_f = \pm 1600 \text{ Hz} / 4257 \text{ Hz/Gauss} \times 0.5 \text{ Gauss/cm} = 7.51 \text{ cm}$$

Clearly, if G_f is increased, then FOV_f will decrease.

Intuitively, we see that the spatial resolution along this axis must be related to the distance covered in this image dimension (FOV_f) and the number of data points describing this dimension. From Equations [8] and [9], the pixel size along the frequency encoding axis (FOV_f/N_f) may be derived, giving:

$$[10] \qquad FOV_f / N_f = 1 / (\gamma G_f T)^\dagger$$

The factor of two in the definition of pixel size results from the fact that half of the points after FT only give additional phase information. Equation [10] shows that there are two ways to increase the resolution: (a) increase G_f, causing FOV_f to decrease, or (b) increase both N_f and T by the same factor which leaves BW and FOV_f unchanged.

* A complex point of measured signal consists of two numbers which describe the vector components along each of the two principle axes.

† Rather than sampling frequencies between 0 and 32 kHz, quadrature phase detection allows examination of frequencies from –16 kHz to +16 kHz relative to the local oscillator frequency.

CONTINUED

Phase Encoding

The process of frequency encoding yields, after FT, a projection of the image plane onto the read axis. As stated in the section on Fourier transformation, three pieces of information are conserved: frequency, amplitude and phase. In the projection, variations in frequency denote position along the read axis. And variations in amplitude yield information on the total signal intensity contained in the column represented by each point along the projection. Note, however, that variation in phase has not thus far been used to provide image information. In order to produce a two-dimensional image of the slice, one could cause a systematic variation in phase which would encode the spatial information along the one remaining principal axis of the image plane.

(FIG. 25) shows a complete 2D-imaging pulse sequence. The only addition to the pulse sequence relative to that considered previously is a single gradient pulse on the third gradient axis (phase encoding axis). Since this phase encoding gradient is not on within the acquisition window, it cannot affect the detected frequencies. However, as we have seen previously, the phase change of transverse magnetization due to this gradient pulse will be preserved in the form of phase memory. The induced phase change is proportional to the amplitude and duration of the gradient times the position of spins along that axis.

Implementation of phase encoding is accomplished as follows. The complete pulse sequence is played out many times (typically 128 or 256 times) and the resulting signals are stored separately. The only variation from one acquisition to the next is the amplitude the phase encoding gradient which is changed in a step-v fashion. Separate Fourier transformation of each of the data sets ("views") yields a set projections onto the read axis These projections are expectedly identical to one another with respect to frequency but not with respect to phase.

If this were x-ray CT, collecting a set of views which we all projections onto the *same* axis would be a pointless exercise.

CONTINUED

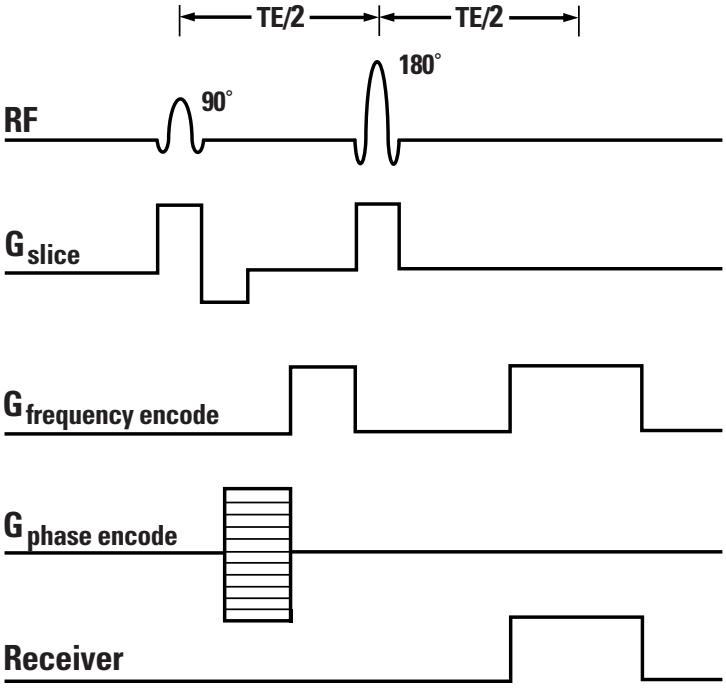

FIGURE 25 – The final dimension of spatial information is obtained by phase encoding. Each view is obtained using a different amplitude for the phase encoding gradient lobe. The action of this gradient is still "remembered" at echo time as phase memory.

BACK

However, if one were to choose any given position of one of these MR views, and then follow the phase at that point progressing from view view to view, variation would be noted. This variation is another interference pattern. Following a different point from view to view reveals a different interference pattern. Since the only change in the pulse sequence from view to view is the amplitude of the phase encoding gradient, the noted interference patterns reflect the sum of phase changes along the phase encoding axis. Another set of FTs is certainly indicated.

A data set consisting of the first point from every projection is constructed and subjected to FT (**FIG. 26**). Another data set is assembled from the second point on every projection, Fourier transformed and stored separately. Then, all of the third points are used, etc. The result is a 3D plot of signal amplitude versus location on the frequency and phase encoding axis. If amplitudes are converted to gray scale, the result is the image of the slice.

Finally, let us consider phase encoding quantitatively. A data set formed by taking the same data point from each of a set of views, represents a discrete digital sampling of an interference pattern. Therefore, the same sampling theory principles which were applied in the frequency encoding dimension, also need to be considered for phase encoding. Specifically, the requirement for sampling at least twice per cycle must be met. To phase encode one cycle requires a 360° phase change, necessitating at least one sample for every 180° phase change. This means that the two edges of the FOV in the phase encoding dimension correspond to those positions along the phase encoding gradient axis when each incremental change in the gradient amplitude causes a 180° phase change. At positions between these two points, the phase changes by less than 180 ° per view. In analogy to Equation **[8]** we can write:

$$\gamma G_P * FOV_P * T_P = N_P * \pi \quad [11]$$

where N_p is the number of phase encodings (views), T_p is the duration of the phase encoding gradient pulse, FOV_p is the FOV in the phase encoding dimension and G_p is the maximum amplitude of the phase encoding gradient.

CONTINUED

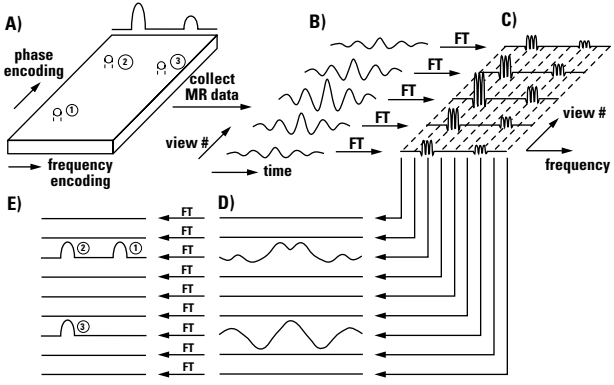

FIGURE 26 – Schematic representation of image formation by 2D-FT. (A) This represents a slice through an object containing 3 vials of water (labeled 1, 2 and 3). The projection onto the frequency encoding axis is shown behind the slice. (B) Collection of MR data from the slice yields a set of spin echoes (views). Note that each echo is produced from the entire slice. (C) Fourier transformation of all of the views yields a set of projections of the slice onto the frequency encoding axis. The oscillations underneath the envelope of each projection represent one-half of the phase information. (D) A new data set is assembled from the columns in C (added views have been filled in). Some of the rows of the new data set contain no signal because these rows correspond to positions along the frequency encoding axis where there is no water. Two of the depicted rows do contain signal. The lower of these two rows is a signal containing a single frequency, while the upper row is an interference pattern of two sinusoids. (E) FT of all of the rows in D produces the image. The image needs to be rotated and flipped in order to correspond to the slice depicted in A. Note that the data would have a more complex appearance if the vials of water were larger than one pixel each; resonances from one portion of a vial would interfere with resonances from other portions.

BACK

The spatial resolution can be expressed as the pixel size which, in phase encoding direction, is equal to the ratio FOV_p/N_p for which we obtain from Equation [11].

$$[12] \qquad FOV_P / N_P = \pi / (\gamma G_P T)$$

Hence, we can lower pixel size by increasing the amplitude of the phase encoding gradient (in analogy to the frequency-encoding gradient which controls the pixel size in the read direction of the image). Alternatively, however, we can increase the duration of the phase encoding gradient.

Reconstruction

Reconstruction is a term brought to MR from CT, where it refers to projection reconstruction which is the mathematical process used to transform raw data into a CT image. As we have seen, the two-dimensional Fourier transform method used in MR is a very different kind of process than projection reconstruction.

In MR, the word "reconstruction" has a more general connotation, and denotes all of the computer processing interposed between raw data and image. The 2D-FFT is central to this processing, but it also includes baseline corrections, mathematical weighting of the raw data for artifact reduction and other purposes, post-2D-FFT data filtering for edge enhancement or smoothing, magnitude calculation, corrections for gradient imperfections, scaling for image processing, and image reorientation (rotating, and flipping) for a standardized presentation format.

Let us follow the processing from raw data to image for an MR image. (FIG. 27A) shows the raw data for the image in (FIG. 27C), while (FIG. 27B) shows an intermediate step after the first dimension of FT, i.e. all of the views have been transformed in frequency-encoding direction. In all three figures the phase information has been discarded; the brightness at each point represents signal amplitude. High signal is represented as white (note that this is the opposite of the convention used in CT, where white means high attenuation).

CONTINUED

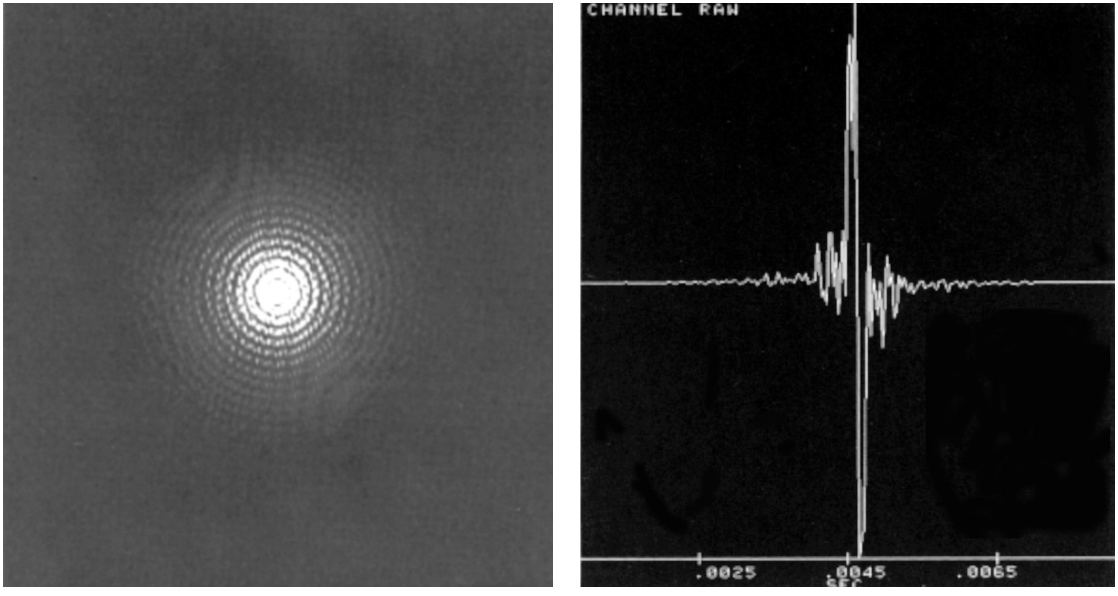

FIGURE 27A – Reconstruction. (A) This is the not-so-mysterious k-space data or raw data. Each view is a spin echo; the middle views have the greatest amplitude because they were obtained with the weakest amplitudes of the phase encoding gradient.

BACK

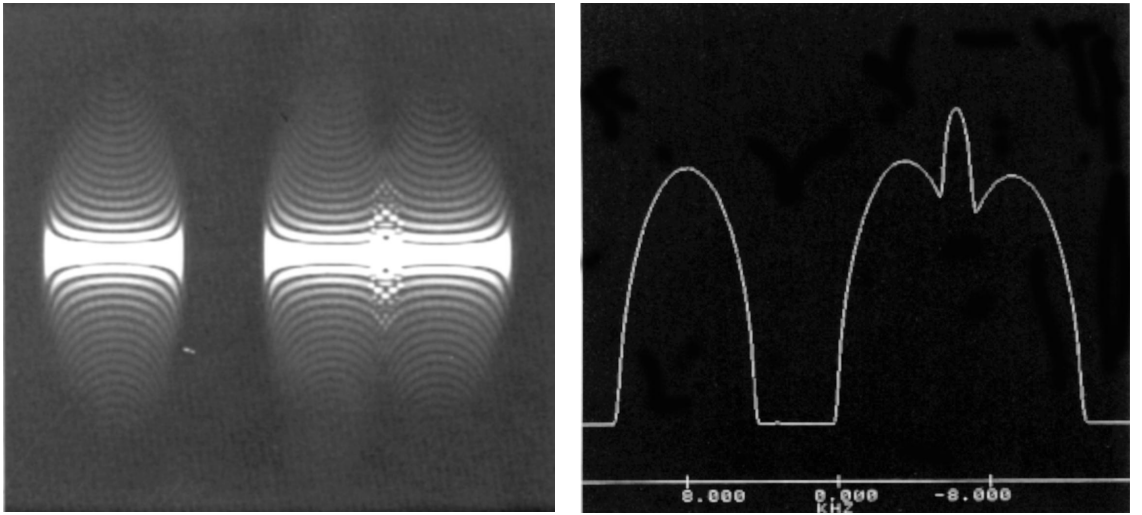

FIGURE 27B – Reconstruction. (B) The FT of any one of the views gives a projection onto the frequency encoding axis. View No. 128 is displayed on the right.

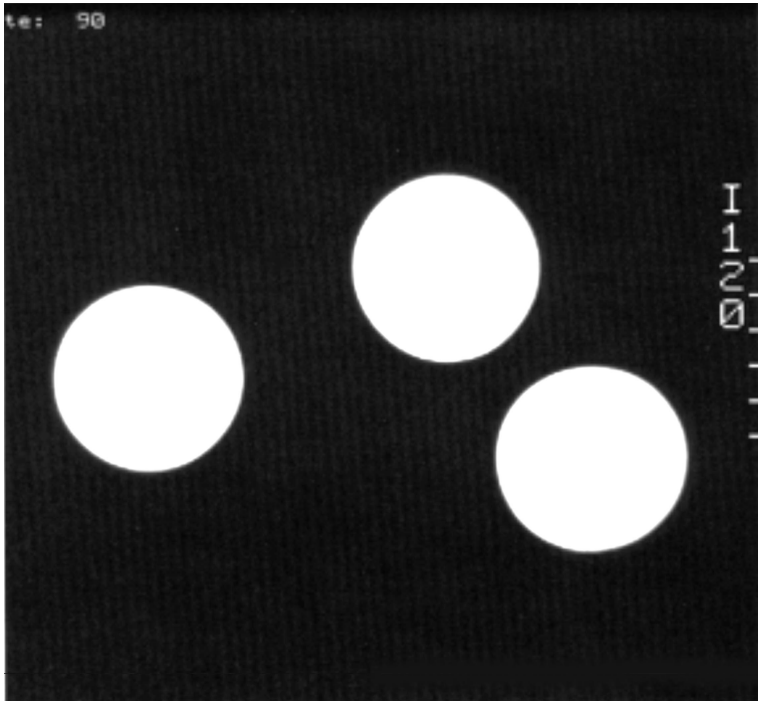

FIGURE 27c – Reconstruction. (C) The second dimension of FTs yields the image.

BACK

Multislice Acquisition

Thus far the acquisition of image data for only a single slice has been considered. The question naturally arises: How much time is needed to acquire these data? The answer is:

[13] Total Acquisition Time = Number of views x Number of excitations per view x TR

The number of views collected for an image is defined by the selected matrix size. Typical matrix sizes are: 256 x 128, 256 x 192, and 256 x 256.

The second number of each pair represents the number of views. Clearly, as discussed in more detail below, if one were to collect all the image data from one slice, and then repeat the entire acquisition for the same slice, the two data sets could be added together in order to gain SNR. This is the process which is alluded to by the term "Number of excitations per view," also abbreviated as NEX. A typical set of imaging parameters might be: TR = 1000 ms, TE = 25 ms, NEX = 2, Matrix = 256 x 128.

The total acquisition time for one image (slice) would be 128 views x 2 excitations per view x 1000 ms per excitation = 256,000 ms = 256 sec = 4 min 16 sec

Does this mean that using this protocol would require 8 min 32 sec to acquire data for two slices, and 12 min 48 sec for three images? This would be quite uneconomical since TE is much shorter than TR, implying that almost all of the duration of TR is "dead time" waiting for T1 processes to restore longitudinal magnetization in the excited slice. During this dead time, we may be exciting and detecting a different slice parallel to the first slice. In fact, as illustrated in (**FIG. 28**), excitation/detection may be carried out in many parallel slices during each TR interval. There is easily enough time in the above example to collect data from more than 20 different slices during the 1000 ms TR interval. Thus, image data from at least 20 different slices can be collected in the same 4 min 16 sec calculated above for one slice.

CONTINUED

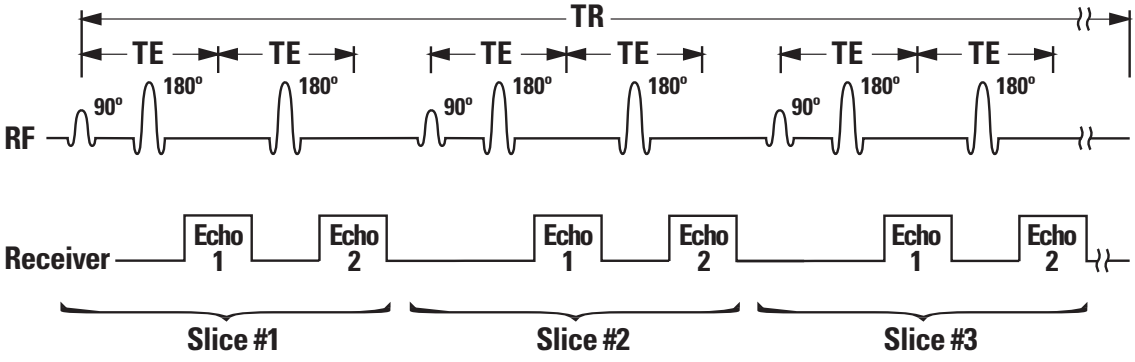

FIGURE 28 – Interleaved multislice acquisition. Since TR is usually longer than the time required for excitation and detection in a slice, the remaining time within each TR interval may be used for excitation/detection in other slices.

BACK

CONTRAST

The intensity or brightness at any given position in an MR image reflects the amplitude of the MR signal arising from that position, which in turn is proportional to the concentration of mobile protons (proton density, abbr. N(H)) in that region. If imaging parameters are selected which cause image intensity to reflect only variations in N(H) across the image, the image is termed a proton density image. An example of this is shown in (**FIG. 29**). The image has a rather "flat" appearance, i.e. the intensity does not vary much from structure to structure. The reason for this appearance is that N(H) does not vary greatly in different tissues. Therefore, it is desirable to seek other sources of contrast which vary more significantly from tissue to tissue; the relaxation times T1 and T2 are good candidates for sources of contrast. In the following we will examine extreme cases of contrast (**REF. 12**).

Suppose there were two adjacent tissues of equal mobile proton density but possessing different relaxation characteristics. Both tissues would be subjected to a long train of spin-echo sequences, just as in image data collection. The two important operator controlled acquisition parameters involved are TR and TE.

CASE 1: TR is very long (TR >> T1) and TE is very short (TE << T2). Since TR is very long, both tissues completely recover all of their longitudinal magnetization between each spin-echo excitation/detection sequence, even though the two tissues possess different T1 values. Therefore, differences in T1 values will not affect the amount of longitudinal magnetization which is available for a subsequent spin-echo in the train. We have also assumed that the two tissues possess different T2 values. Remembering that T2 relaxation describes the rate of decay of signal in the transverse plane, a long TE would yield different amounts of signal from tissues possessing different T2s. However, in this case TE is very short so the signal from neither tissue has time for much decay at all. Thus, neither differences in T1 nor differences in T2 will effect signal intensity. These conditions yield a proton density image (**FIG. 29**). The two tissues will appear isointense due to their equal N(H) values.

CONTINUED

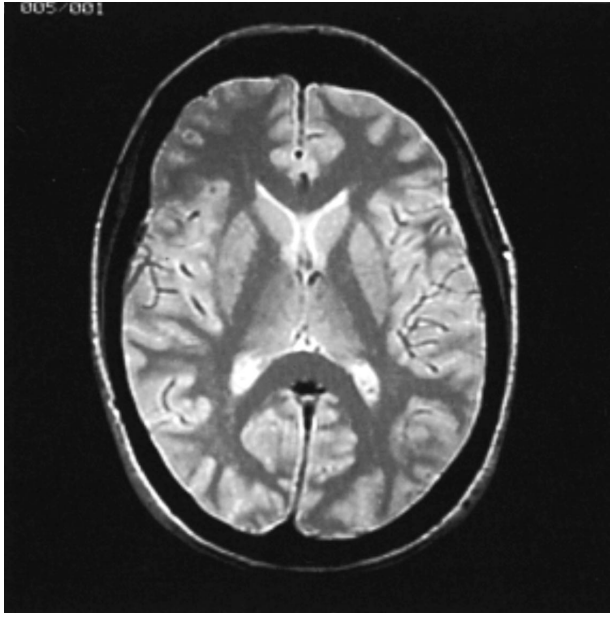

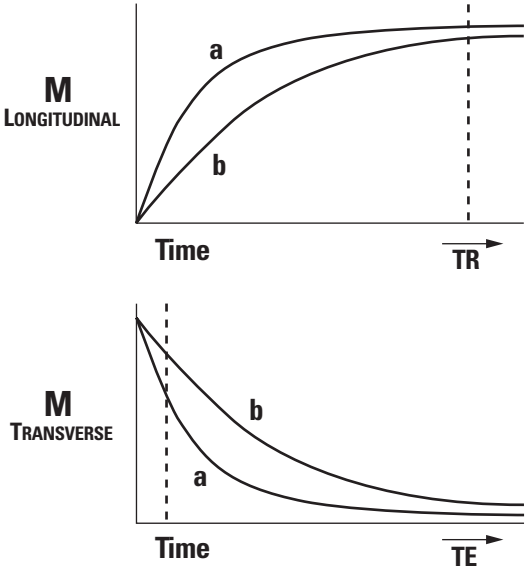

FIGURE 29 – Proton density weighted images are obtained by using a long TR and a short TE (TR = 6000 ms, TE = 20 ms). Note the rather uniform intensity across the various brain structures. On the graphs, two tissues with differing relaxation characteristics are indicated as a and b.

BACK

CASE 2: TR is still very long but TE is prolonged to the range of tissue T2 values. As in Case 1, the very long TR permits complete recovery of longitudinal magnetization in both tissues between each spin-echo sequence, regardless of variations in tissue T1 values. Unlike the previous case, however, T2 differences will be reflected in signal amplitudes. Since the signal is not detected until the time TE after the 90° pulse, the transverse magnetization from the short T2 tissue will have decayed to a greater extent than that arising from the long T2 tissue. Thus, the long T2 tissue contributes more signal, causing it to appear hyperintense in the MR image relative to the short T2 tissue. This is termed a T2 image or more properly, a"T2-weighted image" since in practice TR is not infinitely long Note that proton density is still a factor: if the tissue T2 values are equal, clearly a tissue with the greater N(H) will be brighter than others even on a T2 image. (**FIG. 30**) demonstrates the concept of T2 weighting.

CASE 3: Now TR is shortened (to the range of tissue T1s), and TE is very short (TE << T2). As in Case 1 above, the very short TE does not allow time for significant decay of transverse magnetization, so that T2 variations do not affect signal intensities. However, since TR is short, the amount of longitudinal magnetization present immediately before each spin-echo excitation/detection sequence depends on how fast it recovered from the previous excitation pulse. A tissue with a short T1 value then has more longitudinal magnetization available for conversion into transverse magnetization on each excitation. Thus, the tissue exhibiting the shorter T1 value yields more signal and appears hyperintense relative to the longer T1 tissue. The applied TR and TE times set forth in this case yield a T, or T1-weighted image. Again, intensity variations are still expected for variations in N(H). (**FIG. 31**) shows T1 weighting

CASE 4: Both TR and TE have values comparable to T1 and T2, respectively. This yields mixed T1 and T2 weighting More specifically, given the variations of relaxation times for different anatomic structures, the contrast is actually indeterminant. This situation is generally (but not always) avoided.

CONTINUED

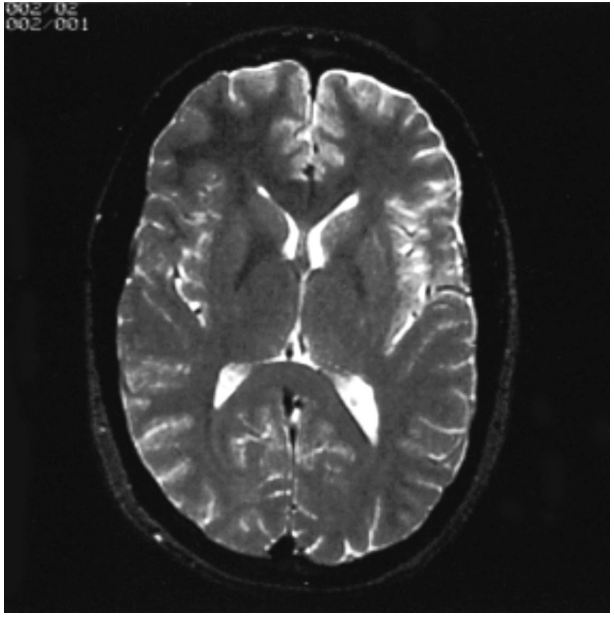

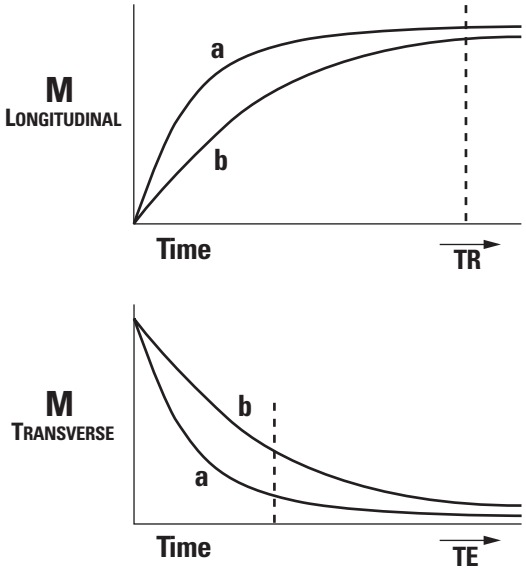

FIGURE 30 – T2 weighting is accomplished with a long TR and an intermediate TE. For both T1 and T2: CSF > gray matter > white matter > subcutaneous fat. For this reason CSF shows the greatest intensity and fat the least. (TR = 4000 ms and TE = 80 ms).

BACK

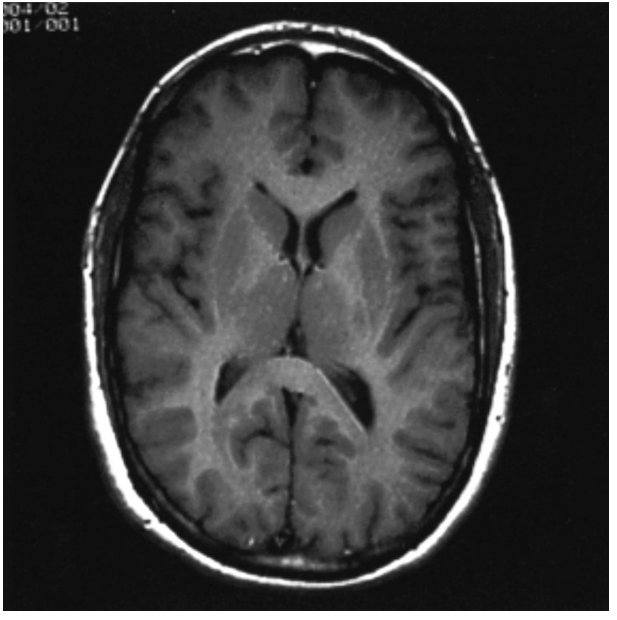

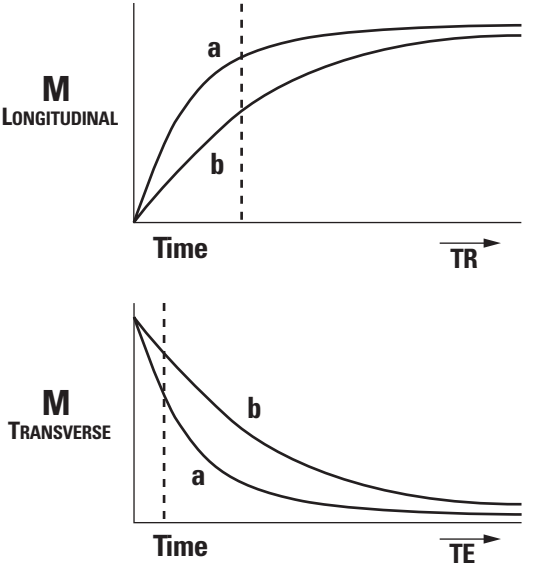

FIGURE 31 – Employment of a short TE and intermediate TR confers T1 weighting. (TR = 400 ms, TE = 20 ms.) Long relaxation time structures are now hypointense.

BACK

Moreover, short TRs used together with long TEs lead to an overall decrease in signal intensity.

In summary, TR controls T1 weighting and TE controls T2 weighting. Short T2 tissues are dark on T2 images, but short T1 tissues are bright on T1 images. (**TABLE 3**) gives an unrealistic but didactically useful summary of these concepts for extremes of contrast.

Parameters Influencing the Signal-to-Noise Ratio (SNR) and Spatial Resolution

Let us consider acquisition of a T1 weighted image using, for example, TR = 600 ms and TE = 20 ms. Upon examination of the image, it may be decided that SNR is too low, suggesting alteration of the imaging parameters with the purpose of increasing SNR. One could increase TR, permitting more longitudinal magnetization to build up between each spin-echo excitation/detection sequence. This would result in increased signal and improved SNR versus the first image, but as implied in the previous section, *the contrast would also change.* In order to make useful comparisons of image SNRs, the contrast must be held constant.

There are three interacting quantities to be considered (**FIG. 32**): acquisition time, sensitivity and spatial resolution. In the following; it will become apparent that any one of these quantities may be improved at the expense of one or both of the other two. Since TR and TE are held constant, the total acquisition time will be dictated by the number of views acquired per image and the number of excitations per view (NEX). Sensitivity may be improved at the expense of acquisition time by increasing the NEX; spatial resolution will be unchanged. Using multiple NEX is equivalent to signal averaging wherein SNR increases proportional to the square root of NEX. Thus, if two images are acquired under identical conditions, except that 2 NEX are employed for image "A" and 8 NEX for image "B,' the acquisition time for B would be four times that of A. But SNR for B would be only two times that of A. Although time was traded for SNR, it was not an even trade.

CONTINUED

TR	TE	CONTRAST
>>T1	<<T2	N(H)
>>TR1	~T2	T2
~T1	<<T2	T1
~T1	~T2	MIXED

TABLE 3 – Contrast extremes for spin echoes

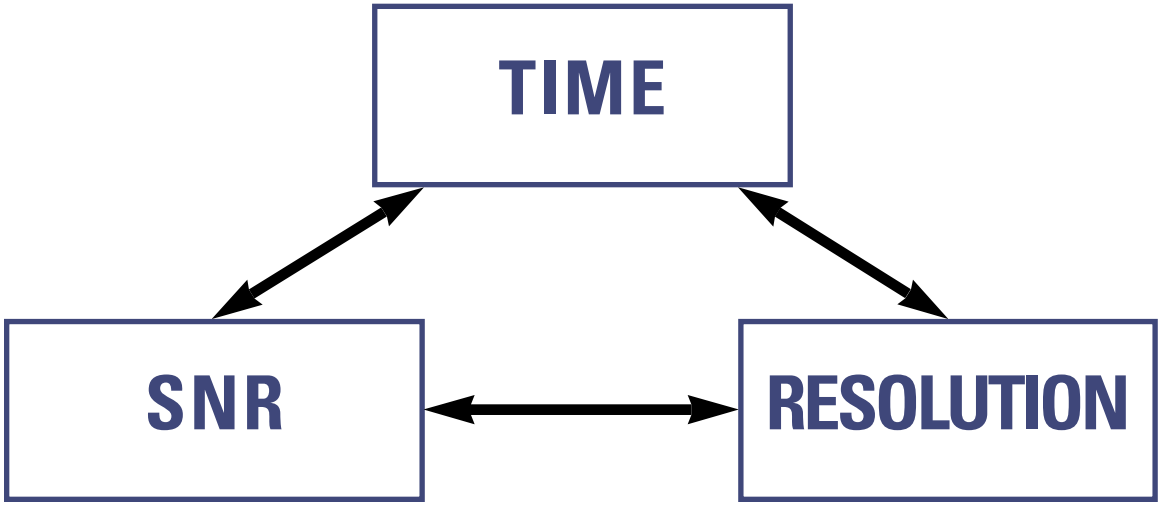

FIGURE 32 – This paradigm illustrates the inter-relatedness of the three qualities. Improvement of one of three is at the expense of one or both of the other two.

BACK

The concept of a "voxel" is useful for discussing the tradeoff between spatial resolution and sensitivity. A voxel is defined as the volume element in the body corresponding to one picture element or pixel in the image. The dimensions of a voxel are:

$$d_{sl}\ (FOV/N_p)(FOV/N_f)$$

Note that the last two terms reflect the FOV in both dimensions divided by the matrix size in both dimensions. The voxel concept provides a mechanism for stating general rules on SNR versus resolution. If acquisition parameters are changed such that each voxel is made larger, then there are more spins in each voxel to contribute to the signal; this increases SNR. By the same token, larger voxels imply a decrease in spatial resolution. The converse is also true. Smaller voxels yield decreased SNR but increased spatial resolution.

Given the voxel dimensions defined above, the operator-controlled parameters that can manipulate the voxel size are: slice thickness, FOV and matrix size. If, for example, the slice thickness is decreased by a factor of two, the volume of each voxel is halved, which in turn yields 1/2 the SNR and twice the spatial resolution (along the slice axis). If the FOV is halved, this decreases the voxel size by a factor of 4, leading to 1/4 the sensitivity and 2 times the spatial resolution in each of the two dimensions.

The effect of changing matrix size is not as obvious as for FOV and slice thickness. Assume a change from a 256 x 128 matrix to a 256 x 256 matrix, i.e. twice the number of views. The voxel size is decreased by a factor of 2, doubling the spatial resolution in the phase encoding dimension of the image (**FIG. 33**). This increased resolution is purchased with both decreased SNR and double the acquisition time in order to collect twice as many views. Doubling the acquisition time as in the case of doubling NEX, *increases* SNR by the square root of 2 = 1.4, while increasing the resolution by a factor of 2 *decreases* SNR by a factor 2. The overall effect on SNR is a decrease by a factor of 1.4.

CONTINUED

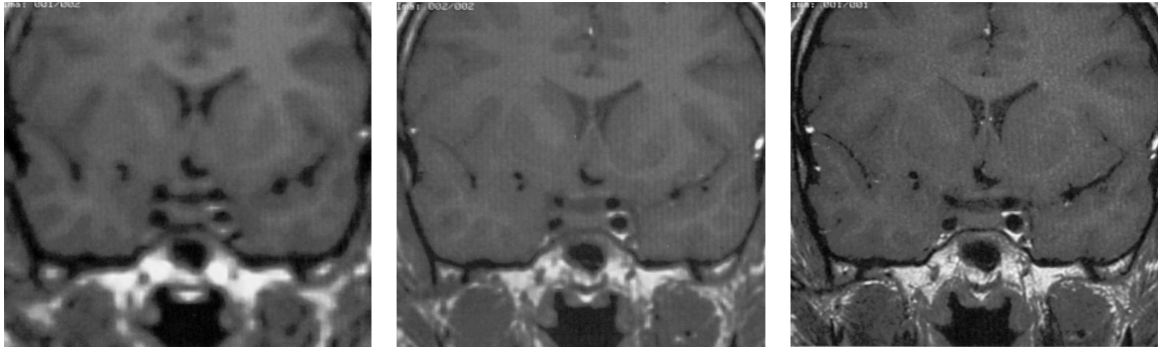

FIGURE 33 – Shown are 3 images acquired at the same location under identical conditions with the exception of variation of FOV and hence voxel size. The images are shown appropriately magnified to show the same regions of tissue. As the FOV is decreased, spatial resolution increases, but SNR decreases.

BACK

The receiver bandwidth discussed above in the section on frequency encoding, also affects SNR. This may be understood as follows. Noise is assumed to be randomly distributed across all frequencies. There is a certain amount of signal generated by excitation, and with the read gradient we choose the range of frequencies over which to spread the total signal. The greater the range of frequencies, the less signal there can be at any one frequency. Since the same amount of noise is present at all frequencies, SNR decreases with increasing receiver bandwidth. This description is intuitive but not quantitatively accurate. The quantitative relationship is:

$$\mathbf{SNR} \propto \sqrt{1/BW}$$

The wary reader suspects that decreasing BW does not yield free SNR, and considers the price in terms of resolution and/or time. Resolution is indeed decreased but in a different fashion than in the earlier examples. Voxel size is unaffected; however voxel to voxel discrimination in units of frequency decreases. Under the naive assumption that, in the absence of an explicitly imposed magnetic field gradient, all protons resonate at exactly the same frequency, the decrease in voxel frequency discrimination is of little consequence. Although this has been the working assumption throughout this text, it is only true to a degree. If B_0 is in homogeneous over the imaging volume, then the proton resonance frequency is also inhomogeneous. Moreover, protons in different chemical environments, such as those in water versus lipid, resonate at slightly different frequencies at the same B_0 field. Other factors including magnetic susceptibility changes also effect the proton resonance frequency at B_0 field. The ultimate limit of this assumption is T2: since the signal does not persist for an infinitely long period of time, its frequency cannot be determined with an infinite degree of accuracy. Using the 32 KHz bandwidth of an earlier example and given 256 pixels in the frequency encoding dimension, then the discrimination or frequency resolution is 125 Hz/pixel. Uncontrolled variation of the proton resonance frequency which is greater than 125 Hz will cause misregistration, blurring or other image artifacts.

CONTINUED

The innate SNR of magnetic resonance in humans approximately increases linearly with B_0, At higher field strengths the population difference between the two spin energy levels is larger, accounting for the improved SNR. In practice, full advantage of greater B_0 fields is not realized, in part, because T1 is somewhat longer, necessitating the use of longer TRs and also because higher magnetic fields demand larger gradients and thus increased receiver bandwidth. Nevertheless, field strength is a key parameter which very significantly governs the performance of an imager. The more intrinsic SNR available, the more of the excess SNR can be traded for spatial resolution or decreased acquisition time.

Imaging with Gradient Echoes

(FIG. 34) depicts a gradient echo imaging pulse sequence known as GRASS (Gradient Recalled Acquisition at Steady State). Let us first examine features which are familiar from knowledge of spin-echo based imaging. Frequency encoding is accomplished in the same manner; i.e. imposition of the read gradient when the receiver is on. Phase encoding and slice selection are also as in spin-echo imaging.

In contrast to spin-echoes, the GRASS sequence does not employ a 180° RT pulse; furthermore, the single RF pulse used generally yields a flip angle θ of less than 90.° Echo formation is controlled by the action of the gradient along the frequency axis as follows. The RF pulse generates a certain amount of transverse magnetization which is dephased by the first gradient pulse on the frequency axis. The read gradient is of opposite polarity as the dephasing gradient and causes rephasing of the transverse magnetization (FIG. 35). Rephasing is complete when the area (gradient amplitude times duration) of the first gradient pulse is equal to the area of the second gradient pulse. When this condition is fulfilled, the gradient echo has its greatest amplitude; the gradients are adjusted such that this occurs in the middle of the acquisition window. The use of gradient echoes allows for shorter TEs than spin-echoes (5-10 ms).

CONTINUED

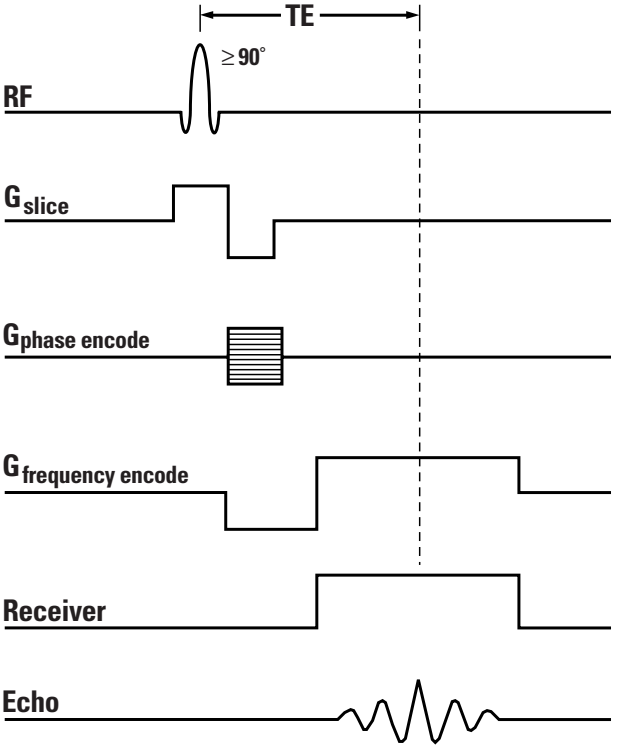

FIGURE 34 – Pulse sequence for gradient echo imaging.

BACK

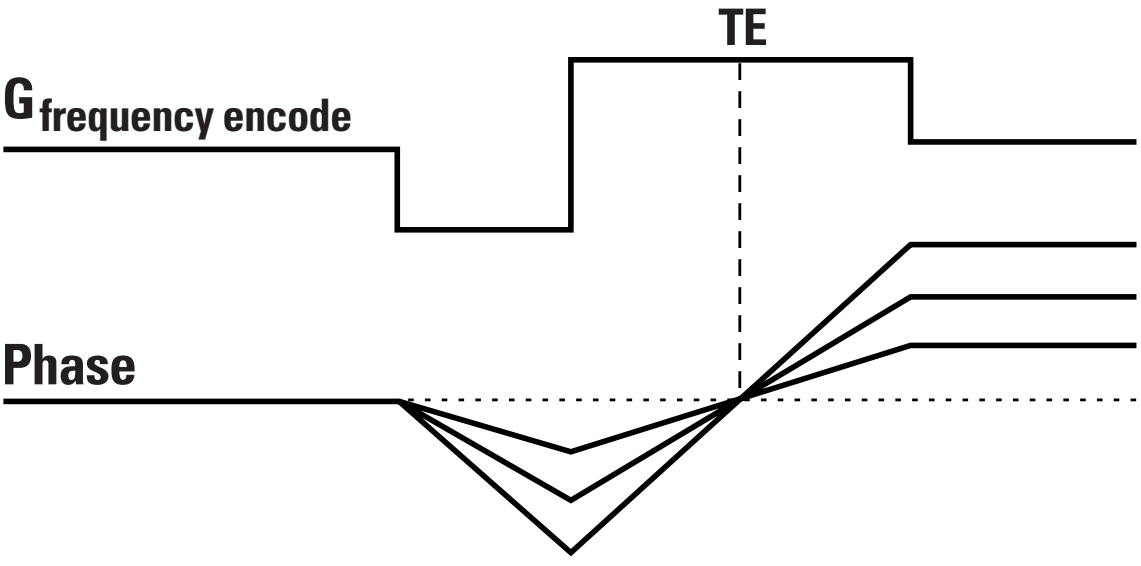

FIGURE 35 – This illustrates the mechanism of gradient echo formation. The first gradient lobe dephases transverse magnetization along the frequency encode axis, then the first half of the read gradient refocuses the magnetization giving an echo at time TE. The phase plot shows the effect on magnetization at four different locations along the frequency encode axis (FIGURE 19).

BACK

Gradient echoes do not refocus dephasing due to B_0 inhomogeneity as spin-echoes do, and yield increased artifactual responses to magnetic susceptibility variations. Thus, in GRASS imaging, signal intensity for a given TE is a function of T*2 rather than T2 (**REF. 13**).

At first, it might seem disadvantageous to use a flip angle which is less than 90° (**FIG. 36**). This converts only a fraction of the longitudinal magnetization into transverse magnetization to be detected. However, if short TRs are employed with a train of gradient echo excitation/ detection sequences, then smaller flip angles result in more longitudinal magnetization available for each excitation.

Contrast phenomenology using gradient echoes is complicated by the addition of two new factors. The first of these is that it is possible to "re-use" transverse magnetization. If TR is very short, i.e. in the same range as T2*, then a certain fraction of the transverse magnetization generated by an excitation is returned to the longitudinal axis by the next excitation (steady-state free precession phenomenon). The net effect of this recycling of transverse magnetization is increased signal intensity for long T2 (and thus also long T2*) structures.

The second new factor is the addition of the operator controlled variable θ, which together with TR and TE determine the observed image contrast (**TABLE 4**). If TR is significantly longer than T2* (TR > 200 ms) so that the aforementioned magnetization recycling is not effective, then decreasing ø is equivalent to increasing TR for the contrast extremes discussed for spin-echoes. Low θ values increase proton density weighting, while high θ values increase T1 weighting, all at a given TE. At very short T2's, however, the images become weighted toward T2/T1, i.e. structures with a larger T2/T1 ratio (liquids) appear bright.

The often used very short TRs preclude an interleaved multi-slice acquisition as discussed for spin-echo imaging; there simply is not enough time within TR for excitation/detection in other slices. The GRASS pulse sequence executes a sequential acquisition of image data for the chosen number of slices.

CONTINUED

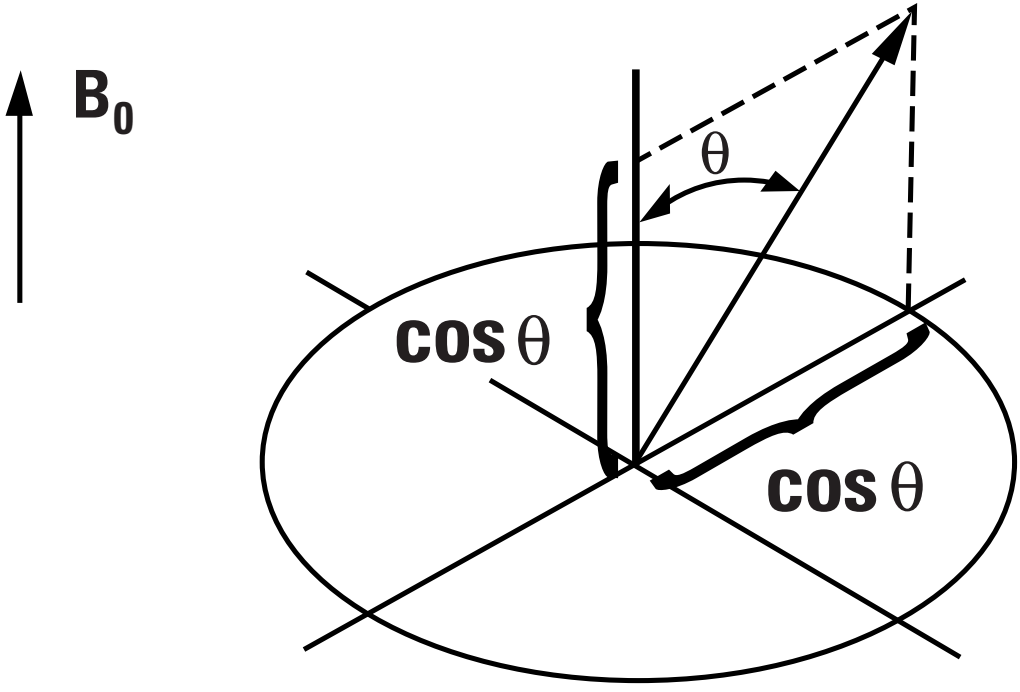

FIGURE 36 – Use of a flip angle θ which is less than 90°. This can conserve longitudinal magnetization. For example, if θ = 30° then 87% of the magnetization is left longitudinal, and transverse magnetization is decreased by only a factor of 2.

BACK

DOMINANT CONTRAST				
	T1	T2* (1)	N(H) (2)	
TR (ms)	200-400	20-50	200-400	200-400
TE (ms)	8-15	8-15	30-60	8-15
0 (deg.)	45-90	30-60	5-20	5-20

TABLE 4 – Contrast characteristics of GRASS images

(1) Somewhat T2* weighted
(2) HeavilyT2* weighted

BACK

In this regime, the total acquisition time is directly proportional to the number of prescribed slices:

[14] Total Acquisition Time = Number of slices x Number of views per slice x NEX x TR

Another gradient echo pulse sequence (denoted MPGR) which is intended for use with longer TRs (hundreds of milliseconds), executes an interleaved slice acquisition. (FIG. 37AB) & (FIG. 37CD)

3D-Gradient Echo Imaging

The essential idea in 3D-FT imaging is the replacement of slice selective excitation with another phase encoding process along the slice axis (FIG. 38). Each RF pulse excites the entire imaging volume instead of just one slice. The slice information is obtained by accumulating the data as before for all the views and then incrementing the amplitude of the slice encoding gradient, and then repeating the acquisition of all the views. This process is repeated usually 32 to 128 times; 3D-FFT of the 3D data set then yields 32 to 128 images.

In practice, it is often desirable to limit the 3D-acquisition to just a portion of the volume of the RF coil. This is accomplished by selecting a slab encompassing the slices to be imaged. The 3D-acquisition then results in subdividing the slab into thinner slices. (FIG. 39)

3D-imaging permits us to obtain very thin contiguous slices with minimal interslice cross-talk. Since information is obtained for the entire imaging volume on every view, the SNR is greater than for a comparable 2D-sequential imaging method, e.g GRASS. The SNR improvement is proportional to the square-root of the number of slices, making it attractive to collect data corresponding to a large number of slices (which also decreases interslice cross-talk). The contrast for a 3D acquisition is the same as that for a comparable 2D acquisition.

What length of time is required to acquire a 3D data set? It is the same as for short TR GRASS:

[14] Total Acquisition Time = Number of slices x Number of views per slice x NEX x TR

CONTINUED

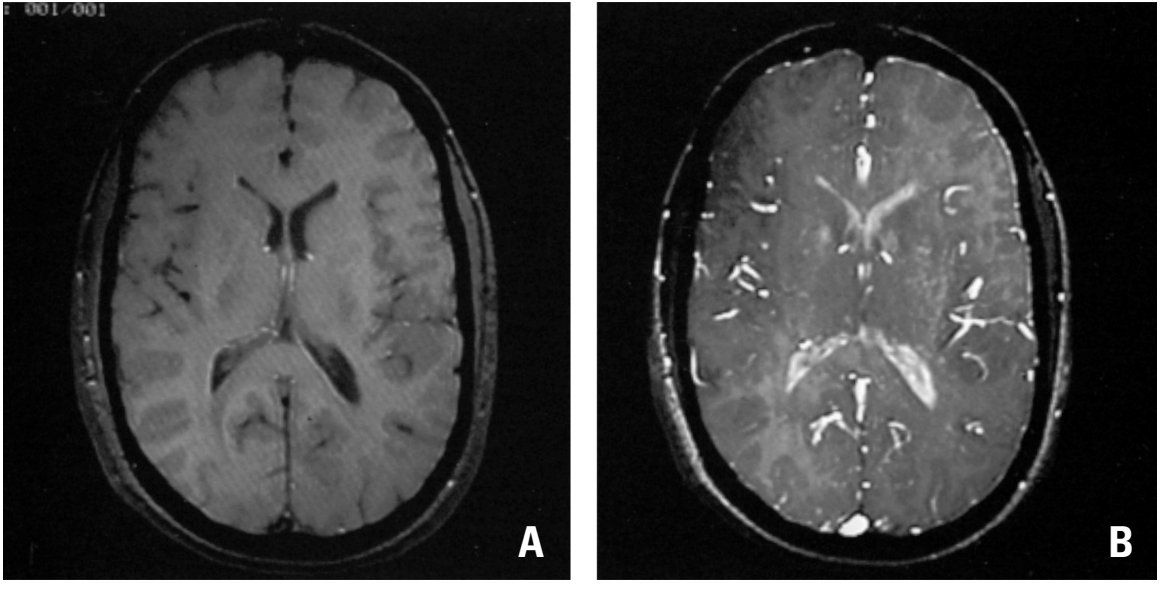

FIGURE 37AB – These GRASS images show types of contrast obtained with variation of θ TR and TE: (A) TR = 300 ms, TE = 13 ms, θ = 60°, T1 weighted, (B) TR = 30 ms, TE = 13 ms, θ = 60°, T2* weighted.

BACK

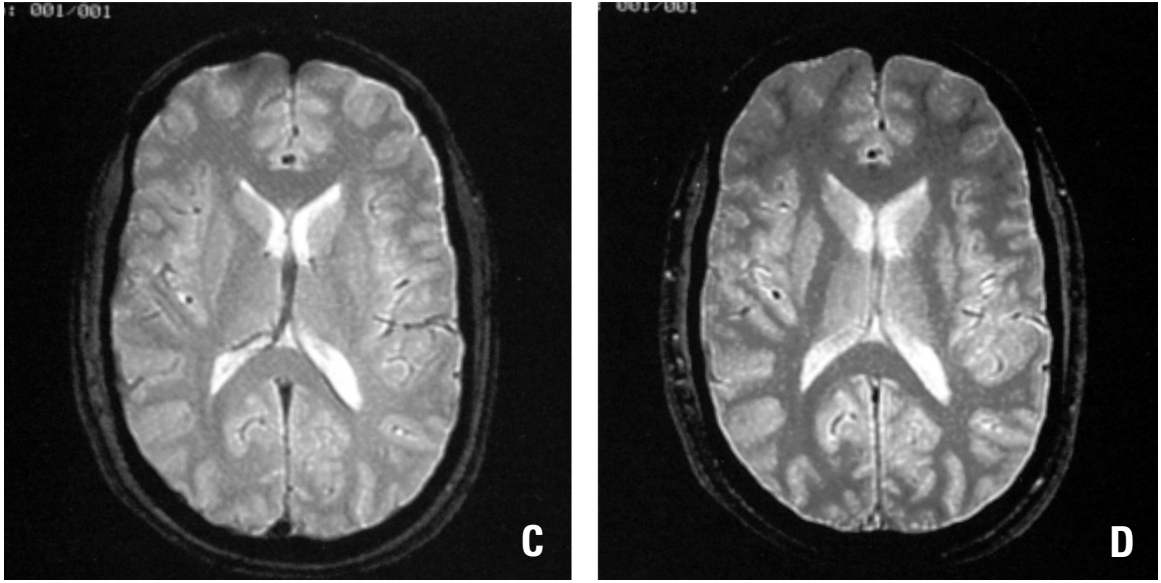

FIGURE 37CD – These GRASS images show types of contrast obtained with variation of θ TR and TE: (C) TR = 300 ms, TE = 35 ms, θ = 15° also T2* weighted, (D) TR = 400 ms, TE = 13 ms, θ = 10° Np weighted.

BACK

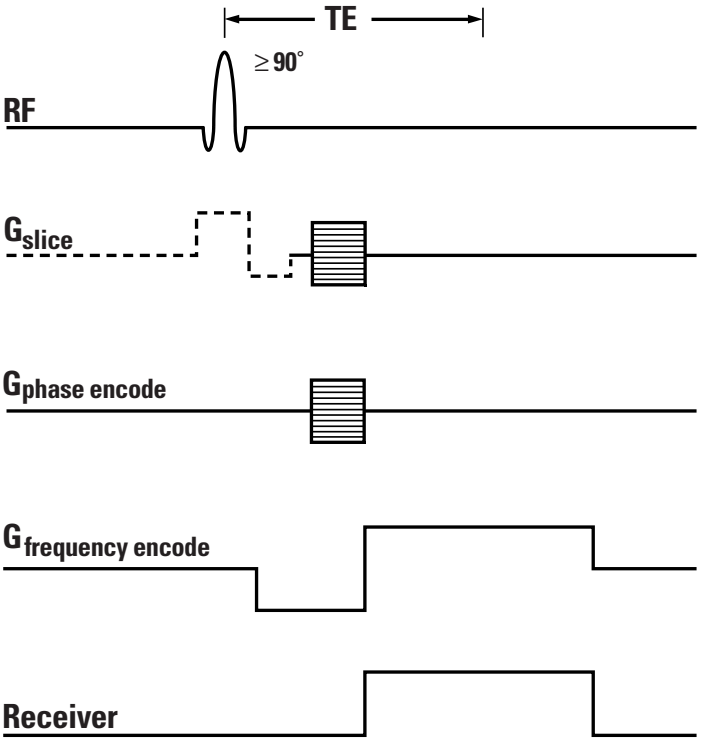

FIGURE 38 – This is the pulse sequence for 3D-GRASS imaging. Here the slice axis is also phase encoded. Slab selective excitation may be employed in order to limit the field of view in the slice dimension.

BACK

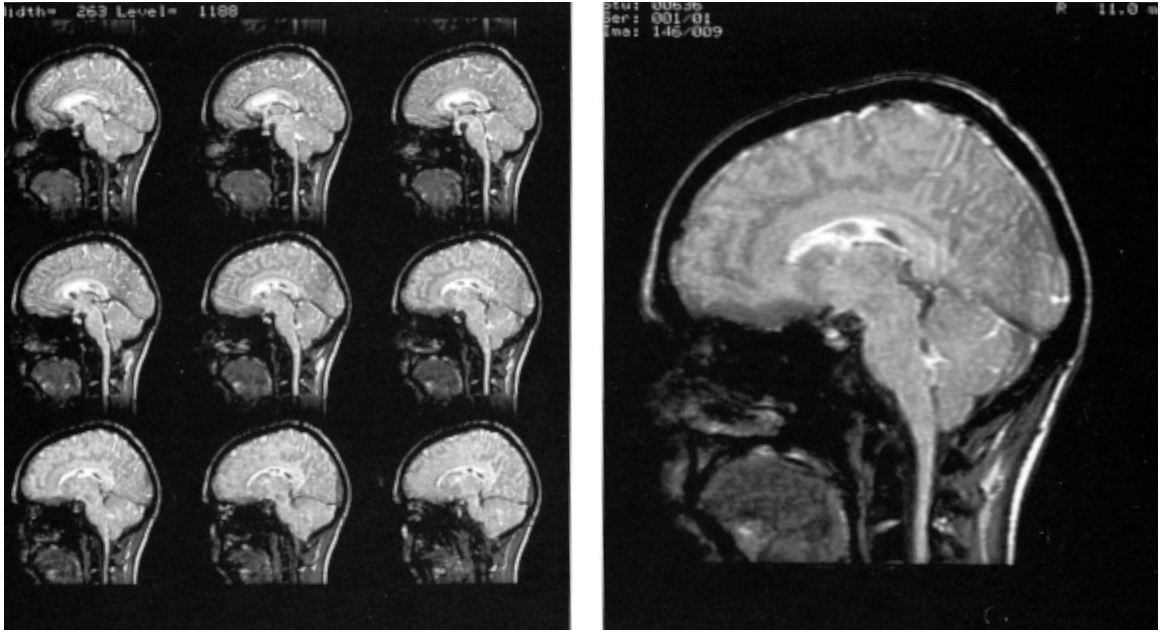

FIGURE 39 – Shown are a few of the 2 mm-thick contiguous slices obtained with 3D-GRASS. The data for 64 images were obtained in 9 min. TR = 33 ms, TE = 13 ms, $\theta = 60°$

BACK

For example, for 64 slices using 256 views, one NEX and TR = 33 ms requires 9 min. figure 33 depicts a few of the images from such an acquisition. 3D-image data sets are often denoted as either *isotropic* or *anisotropic*. These terms refer to voxel dimensions. If all three dimensions of the voxel are equal, say 1 mm x 1 mm x 1 mm, then the data set is termed isotropic. If, however, the three dimensions are not all of equal length, the data are anisotropic. This issue is of relevance when reformatting a set of images. Suppose a set of thin contiguous axial images has been acquired; the image data may be rearranged to yield sets of sagittal, coronal or obliques images. This is another benefit of 3D-imaging which has not yet been fully explored.

Acknowledgment

The author is grateful to Dr. Burton P. Drayer of the Barrow Neurological Institute of St. Joseph's Hospital and Medical Center for helpful criticism. Dr. Felix Wehrli of GE Medical Systems is also to be thanked for his reviews, corrections and skillful editing.

CONTINUED

Bibliography

Principles of Magnetic Resonance

1. Abragam, A. *Principles of Nuclear Magnetism*, Oxford University Press (Clarendon), London, 1961.
2. Slichter, C.P. *Principles of Magnetic Resonance*, 2nd Edition, Springer-Verlag, New York, 1978.
3. Ernst, R.R., Bodenhausen, G., and Wokaun, A. *Principles of Nuclear Magnetic Resonance in One and Two Dimensions*, Oxford University Press (Clarendon) London, 1987.
4. Shaw, D. *Fourier Transform NMR Spectroscopy*, Elsevier, Amsterdam, 1976.

Imaging Principles, Techniques, and Instrumentation

5. Mansfield, P., and Morris, P.G. *NMR Imaging in Biomedicine*, Academic Press, New York, 1982.
6. Morris, P.G. *Nuclear Magnetic Resonance Imaging in Medicine and Biology*, Oxford University Press (Clarendon), London, 1986.
7. Wehrli, F.W.
8. *Nuclear Magnetic Resonance (NMR) Imaging*, Eds. C.L. Partain, A.E. James, F.D. Rollo and R.R. Price, Saunders Co., Philadelphia, 1983.

CONTINUED

9. Henkelman, R.M., and Bronskill, M.J.. "Artifacts in Magnetic Resonance Imaging," in *Reviews of Magnetic Resonance Imaging*, Vol. 2, No. 1, Pergamon, 1987.

10. Bushong, S.C. *Magnetic Resonance Imaging: Physical and Biological Principles*, C.V. Mosby Co., 1988.

11. Bottomley, P.A., Foster, T.H., Argersinger, R.E. and Pfiefer, L.M. "A review of normal tissue hydrogen NMR relaxation times and relaxation mechanisms from 1-100 MHz: Dependence on tissue type, NMR frequency, temperature, species, excision, and age", *Med. Phys.*, 11, 425, 1984.

12. Wehrli, F.W., MacFall, J.R., Shutts, D., Berger, R. and Herfkens, R.J.., "Mechanisms of contrast in NMR imaging," *J. Comput. Assist. Tomogr.*, 8, 369, 1984.

13. Wehrli, F.W.. *Introduction to Fast Scan Magnetic Resonance*, published by General Electric Medical Systems, Milwaukee, 1986.

Original Reports of Historical Interest

14. Purcell, E.M., Torrey, H.C. and Pound, R.V. "Resonance Absorption by Nuclear Magnetic Moments in a Solid," *Phys. Rev.*, 69, 37, 1946.

15. Bloch, F., Hansen, WOO., and Packard, M. "Nuclear induction," *Phys. Rev.*, 69, 127, 1946.

16. Hahn, E.L. "Spin Echoes," *Phys. Rev.*, 80, 580, 1950.

17. Cooley, J.W. and Tukey, J.W., "An algorithm for machine calculation of complex Fourier series," *Mathematical Computation*, 19, 297, 1965.

18. Ernst, R.R., and Anderson W.A. "Application of Fourier transform spectroscopy to magnetic resonance," *Rev. Sci. Instr,*. 37, 93, 1966.

19. Damadian, R. "Tumor Detection by Nuclear Magnetic Resonance," *Science 171*, 1151, 1971.

CONTINUED

20. Lauterbur, P.C. “Image Formation by Reduced Local Interactions: Examples Employing Nuclear Magnetic Resonance,” *Nature*, 242, 190, 1973.

21. Mansfield, P., and Grannell, P.K. “NMR “diffraction’ in Solids?” *J.. Phys. C: Solid State Phys.* 6, L422, 1973.

22. Hinshaw, W.S., “Spin Mapping: The Application of Moving Gradients to NMR,” *Phys. Letters 48A*, 78, 1974.

23. Edelstein, W.A., Hutchinson, J.M.S., Johnson, G, and Redpath, T. “Spin warp NMR Imaging and Applications to Human Whole Body Imaging,” *Phys. Med. Biol.* 25, 751, 1980.

CONTINUED

Glossary

Anisotropic: In the context of 3D-imaging, this term indicates non-cubic voxels. (*See Isotropic*)

B_0: Symbol indicating the external static magnetic field.

B_0 Inhomogeneity: Spatial non-uniformity of the strength of the B_0 field.

B_1: Symbol for the magnetic component of RF energy. For MR, B_1 is perpendicular to B_0.

Contrast: Pertaining to the tissue-to-tissue image intensity variations.

FFT: Fast Fourier Transform.

Flip Angle: The angle which magnetization is rotated by the action of an RF pulse. Symbol = θ.

Fourier Transform: A mathematical process which interconverts time and frequency based descriptions of a waveform (abbr. FT).

Frequency Domain: Data which are graphed as frequency versus amplitude.

Frequency Encoding: Method for obtaining spatial information in one dimension, whereby a gradient is on at the same time that the MR signal is being received.

Gauss: Unit of magnetic field strength. 10,000 Gauss = 1 Tesla.

Gradient: A condition where magnetic field strength varies with position. Intentionally applied magnetic field gradients used for imaging cause a linear change of magnetic field strength along one spatial axis.

Gradient Echo: An echo which arises when two gradient lobes of opposite polarity are sequentially imposed along one gradient axis.

CONTINUED

GRASS: A GE version of gradient echo imaging, also called Fast Scan.

Gyromagnetic Ratio: A measure of the strength of the nuclear magnetism for a given type of nucleus. Symbol = γ. For hydrogen $\gamma H = 4257$ Hz/Gauss. (Also called the Magnetogyric ratio.)

Hertz: Unit of frequency (abbr. Hz). 1 Hz = 1 cycle/sec, 1 KHz = 1000 Hz, 1 MHz = 1,000,000 Hz.

Interleaved Multislice Acquisition: A procedure which takes advantage of the dead time within TR after excitation/detection in a slice, by executing excitation/detection sequences in other slices during this dead time.

Isotropic: In the context of 3-D imaging, this refers to the case where all three voxel dimensions are equal.

k-space: Coordinate system of raw image data; corresponds to the FT of an object.

Larmor Equation: Fundamental equation of MR, $F = \gamma B$, defining the relationship of the Larmor frequency to magnetic field strength.

Lattice: Nuclear environment within which exchange of magnetic energy occurs by spin-lattice relaxation.

Longitudinal Axis: A spatial axis running parallel to B_0.

Longitudinal Relaxation Time: (See *T1 relaxation time.*)

Magnetic Moment: A vector quantity describing the magnitude and nuclear axis of nuclear magnetism.

Magnetic Resonance: The response of nuclei to discrete radiation frequencies and magnetic fields which satisfy the Larmor condition.

Nyquist Frequency: The highest frequency which can be digitally represented properly using a given number of points acquired over a certain period of time.

Phase: Describes the degree to which two sine waves of the same frequency are "in sync" with each other; expressed as an angular relationship.

CONTINUED

Phase Coherence: Expresses the degree to which spins are precessing in synchrony.

Phase Encoding: A process of imparting a positionally dependent phase change to transverse magnetization. The amount of this phase change is incremented from view-to-view and forms the basis for obtaining spatial information along one image axis.

Phase Memory: Refers to the fact that phase changes imparted to transverse magnetization are retained over time.

Pixel: Picture element in an image.

Precession: This is gyration of the spin axis about the B_0 axis which occurs at the Larmor frequency.

Proton Density: The tissue concentration of mobile hydrogen atoms.

Pulse Sequence: A set of RF and gradient pulses of defined amplitude and timing, which is usually repeated many times for acquisition of MR image data.

Quantum Mechanics: Physics of the micro-cosmos based on the concept that all physical quantities can exist as discrete quanta only.

Read Gradient: Refers to the gradient which is imposed during the time that the receiver is on.

Reconstruction: A term referring to all of the mathematical data processing interposed between the data as it is acquired and the image. Fourier transformation is central to this process.

Radio Frequency (Radiation): Electromagnetic radiation of a frequency in the same general range as that used for radio transmission (abbr. RF).

Receiver Bandwidth: The range of frequencies which can be received and properly digitized.

RF Bandwidth: The range of frequencies contained within an RF pulse.

Signal-to-Noise Ratio: A measurement of instrumental sensitivity to MR signals relative to background noise (abbr. SNR).

CONTINUED

Slice Selective Excitation: The use of a magnetic field gradient in conjunction with limited bandwidth RF in order to excite nuclear magnetic resonance signals only in a single slice of the imaging volume.

Spatial Resolution: A measurement of how closely spaced two points can be before they are no longer distinguishable as two points rather than one.

Spin-Echo: An MR signal whose maximum amplitude is a function of T2 rather than T2* relaxation. A spin-echo is stimulated by the pulse sequence 90°-TE/2-180°

Spin-lattice Relaxation Time: See *T1 relaxation time.*

Spin-spin Relaxation Time: See *T2 relaxation time.*

Spin Warp: Version of the two-dimensional Fourier transform imaging method.

T1 Relaxation Time: Time constant for the longitudinal magnetization to reach its equilibrium value.

T2 Relaxation Time: Time constant for the transverse magnetization to reach its equilibrium value in a perfectly uniform magnetic field.

T2* Relaxation Time: Time constant observed for transverse magnetization to reach its equilibrium value in an inhomogeneous magnetic field. T2 > T2*.

TE: Abbreviation for echo time. The time interval from the first RF pulse of a pulse sequence to the middle of a spin- echo or a gradient echo.

Tesla: S.I. unit of magnetic field strength. 1 Tesla = 10,000 Gauss.

Time Domain: Data which are graphed as time versus amplitude.

TR: Abbreviation for repetition time. The time interval from the beginning of a pulse sequence until the beginning of the next pulse sequence.

CONTINUED

Transverse Plane: The plane which is perpendicular to the longitudinal axis.

Transverse Relaxation Time: See *T2 relaxation time.*

Vector: A quantity characterized by both a magnitude and a direction; often symbolized with an arrow.

View: A row in a raw data set consisting of an echo which was acquired using a certain phase encoding gradient amplitude.

Voxel: That volume element in an object which corresponds to one pixel in an image.

CONTINUED

GE Medical Systems

General Electric Company reserves the right to make changes in specifications and features shown herein, or discontinue the product described at any time without notice or obligation. Contact your GE Representative for the most current information.

GE Medical Systems – Americas: Fax 414-544-3384
P.O. Box 414, Milwaukee, Wisconsin 53201 U.S.A.
Internet – http://www.ge.com/medical

GE Medical Systems – Europe: Fax 33-1-30-70-94-35
Paris, France

GE Medical Systems – Asia:
Tokyo, Japan – Fax: 81-3-3223-8560
Singapore – Fax: 65-291-7006